Alma Mater Studiorum – Università di Bologna

DOTTORATO DI RICERCA IN

Scienze Mediche Generali e Scienze dei Servizi

Ciclo XXXIII

Settore Concorsuale: 06/A4 - ANATOMIA PATOLOGICA

Settore Scientifico Disciplinare: MED/08 - ANATOMIA PATOLOGICA

TITOLO TESI

Integrated molecular analysis of endometrial carcinoma: translation of biomarker profiles into the clinical practice

Presentata da: Antonio De Leo

Coordinatore Dottorato

Prof. Fabio Piscaglia

Supervisore

Prof. Renato Seracchioli

Co-supervisore

Prof. Claudio Ceccarelli

Esame finale anno 2021

SUMMARY

Abstract

The Cancer Genome Atlas (TCGA) collaborative project identified four distinct prognostic groups of endometrial carcinoma (EC) based on molecular alterations: (i) the ultramutated subtype that encompassed *POLE* exonuclease domain mutated (*POLE*) cases; (ii) the hypermutated subtype, characterized by MisMatch Repair deficiency (MMRd); (iii) the copy-number high subtype, with p53 abnormal/mutated features (p53abn); (iv) the copy-number low subtype, known as No Specific Molecular Profile (NSMP). Translation of the molecular classification of EC into the clinical practice is emerging as a challenge. Surrogate TCGA markers (*POLE* mutation, microsatellite instability/ MMR deficiency, and p53 mutation/alteration) are being investigated as prognostic and predictive markers in the clinical setting. Although the prognostic value of TCGA molecular classification, NSMP (the majority of endometrial cancer cases) present a wide variability in molecular alterations and biological aggressiveness.

The goal of this PhD thesis project is to promote the integration of pathologic-molecular EC classification into the clinical practice. Specific objectives are: (I) to evaluate the prognostic value of conventional ESMO 2016 clinicopathologic criteria for EC; (II) to investigate the feasibility and the prognostic impact of the novel surrogate TCGA molecular classification of EC; (III) to correlate EC histopathologic characteristics with molecular subtypes; (IV) to explore the relevance of *ARID1A* and *CTNNB1* mutations and their predictive-prognostic weight with particular reference to the NSMP group; (V) to integrate ESMO 2016 clinicopathologic risk stratification criteria with molecular subtyping; (VI) to propose a workable and useful "immuno-molecular" algorithm in routine clinical practice for improving risk stratification and patient management. These objectives represent a novel approach for integrated pathologic-molecular EC classification.

In total, samples of 125 EC patients were included. Next-generation sequencing (NGS) and immunohistochemistry (IHC) were used to assign surrogate TCGA groups and to identify molecular alterations of multiple target genes including *POLE, PTEN, ARID1A*, *CTNNB1*/β-catenin, *TP53*. Associations with clinicopathologic parameters, molecular subtype, and outcomes were determined. Surrogate TCGA molecular typing of the 125 EC cases classified tumors into the following groups: 9 (7.2%) *POLE* group, 41 (32.8%) MMRd group, 26 (20.8%) p53abn group, 49 (39.2%) NSMP group. The most heterogeneous group in terms of clinicopathologic features and outcome was the NSMP category. The analysis of *ARID1A* and *CTNNB1*/β-catenin alterations in NSMP carcinomas identified subsets of ECs statistically correlated with specific histopathological parameters and different disease recurrence rates. In particular, NSMP cases with *ARID1A* mutation showed the worst outcome with early recurrence (log-rank p=0.029), while NSMP tumor with *CTNNB1*/β-catenin alteration and *ARID1A* wild-type showed indolent clinicopathologic features and no recurrence. This study indicates for the first time how the identification of *ARID1A* and *CTNNB1*/β-catenin alterations in high-risk EC represents a simple and effective way to characterize NSMP tumor aggressiveness and metastatic potential: integration of molecular analysis with conventional clinicopathologic (ESMO 2016) parameters significantly improves EC prognostic stratification.

Introduction

Epidemiology of endometrial carcinoma

Endometrial carcinoma (EC) is the most common gynecological cancer in the Western countries and represents the fourth most common female cancer (incidence of 10-20/100,000 women), the sixth most common cause of cancer-related death in women [1, 2]. In Italy, about 8,400 new cases are expected annually (5% of all female tumors; third most frequent cancer in women in the 50-69 age group). The estimated lifetime risk of developing endometrial cancer is 1 out of 47 women. 2,516 deaths were recorded in 2018, representing 4% of deaths from cancer in women [3].

The 5 and 10-year survival rates for EC are 79.0% and 77.5% respectively [4]. This suggests that most patients can be considered cured after five disease-free years. The survival rate of EC is similar to that of breast cancer. It ranks fourth highest in 10-year survival rate for common cancers affecting females, though this rate decreases with age. Although this cancer has a favourable prognosis in low-grade and early stage cases, about 15-20% of patients with endometrial cancer have high-risk disease and follow an aggressive clinical course.

The incidence of EC is related to age. Endometrial cancers usually arise in postmenopausal women, and more than 80% present with abnormal (post-menopausal) bleeding, which often permits detection and cure at an early stage. From 2% to 14% of endometrial carcinomas occur in women younger than 40 years. The peak incidence is in the 55- to 65-year-old age group, with a median age of 63 years. The incidence of EC has grown over the last decade which can largely be attributed to ageing of the population, increased life expectancy, increasing rates of obesity, and the use of estrogen-only forms of hormonal replacement therapy (HRT), which was particularly common in the 1960s and 1970s.

Clinicopathologic classification

Endometrial cancer was traditionally classified into two broad subtypes, type 1 and type 2, based on epidemiology, histopathology and clinical behavior by Bokhman in 1983 [5]. Primarily, the histologic subtypes and molecular alterations were not part of the dualistic model. According to this classification, type I tumors are low-grade, estrogen-related, often clinically indolent, endometrioid carcinomas. Type II tumors are non-endometrioid, clinically aggressive carcinomas that are unrelated to estrogen stimulation and include serous and clear cell carcinomas.

Type I endometrial carcinomas account for about 90% of endometrial cancers and arise in a background of chronic estrogen stimulation. Known risk factors for the development of type I EC correlated with unopposed estrogenic stimulation include ovarian dysfunction, polycystic ovarian disease or cortical stromal hyperplasia (stromal thecosis), estrogen-producing or androgen-producing tumors (rare), diabetes mellitus, obesity, metabolic syndrome, and unopposed estrogen in the form of continuous estrogen therapy. Obesity, which encourages the conversion of androstenedione to estrone in adipose tissue via aromatase activity, is strongly associated with this subset of endometrial tumors. Early menarche and late menopause, nulliparity, infertility are other risk factors. Endometrial carcinomas that are associated with unopposed estrogen tend to be well differentiated, mimic normal endometrial glands (hence, the term *endometrioid*) in histologic appearance, and are associated with a favorable prognosis. The presumed pathway to endometrial cancer involves excess estrogen, development of anovulatory endometrium, subsequent atypical hyperplasia/endometrioid intraepithelial neoplasia (EIN) and, ultimately, adenocarcinoma. Predictably, this subset of tumors affects women in their middle to late 50s but encompasses most adenocarcinomas seen in the younger age groups. Type I tumors generally show minimal myometrial invasion, although deep invasion can occur. The prognosis is generally good, with a 5-year survival of 80% or better.

Type II neoplasms represent another, very different, form of endometrial carcinoma. These are characteristically high grade, not related to unopposed estrogenic stimulation and tend to occur in older postmenopausal women. Tumors in this group account for 15–20% of all endometrial carcinomas. Type II category include serous carcinoma, clear cell carcinoma and poorly differentiated carcinomas. They are not usually associated with atypical hyperplasia/ EIN. In contrast, these carcinomas often occur in a background of atrophic endometrium or arise on the surface of a polyp. Serous endometrial intraepithelial carcinoma (SEIC), the putative precursor lesion, is frequently associated with serous carcinoma. These tumors overall have a poorer prognosis than endometrioid tumors (60% 5-years survival), and the factors predisposing to their development are less well-defined. A small proportion of these tumors arise in association with endometrioid carcinomas, indicating independent processes or, more likely, a single tumor that has evolved to develop heterogeneity through multiple pathogenetic pathways.

Subsequent molecular studies supported the dualistic classification. Type 1 carcinomas are associated with estrogen receptor (ER) and progesterone receptor (PR) expression and demonstrate alteration in the *PI3K-AKT* (*PTEN*, *KRAS*, *PIK3CA*) and Wnt (*CTNNB1*) signaling pathways, and mutations in the chromatin remodeling gene *ARID1A*. In addition, type 1 carcinomas frequently show microsatellite instability either due to MLH1 promoter hypermethylation (sporadic) or a germline mutation in DNA mismatch repair (MMR) genes (*MLH1*, *PMS2*, *MSH2*, *MSH6*, Lynch-associated). In contrast, type 2 carcinomas exhibit loss of ER and PR protein expression, recurrent *TP53* mutations, and *HER2* gene amplification.

However, this the dichotomous classification is imperfect, too simplistic and difficult to apply in clinical practice due to the overlap between tumors of both types and the intratumoral heterogeneity. The corresponding histotypes, i.e. endometrioid or serous, are also not clearly separable in practice with some tumors having ambiguous morphology; especially for high-grade carcinomas, interobserver variability in histotype diagnosis is considerable.

Hereditary syndromes

Approximately 5% of endometrial cancer cases can be attributed to an inherited predisposition.

Women with hereditary non-polyposis colorectal carcinoma syndrome (HNPCC), Lynch syndrome, a condition affecting about 1% of the population, have a 70% lifetime risk of endometrial adenocarcinoma; the mean age is approximately 10 to 20 years younger than non-familial occurrences. Endometrial carcinoma is the most common gynecologic cancer associated with Lynch syndrome and may represent "the sentinel cancer" for more than 50% of affected women. Tumors from patients with Lynch syndrome display the microsatellite instability (MSI) phenotype attributed to defects in mismatch repair (MMR) genes (*MLH1*, *PMS2*, *MSH2*, *MSH6*) or, less commonly, *EPCAM* deletions resulting in epigenetic silencing of *MSH2*.

Given the strong association between EC and Lynch syndrome, the screening of EC specimens for abnormalities in the MMR genes has become routine for many institutions [6]. Several recent international guidelines, including the 2014 guidelines from the American College of Obstetricians and Gynecologists (ACOG), the Society of Gynecologic Oncology (SGO) and the 2016 National Comprehensive Cancer Network (NCCN) guidelines recognize the value of the universal tissue testing for all patients with newly diagnosed EC [7-9].

Universal screening for Lynch syndrome in endometrial carcinomas requires a multidisciplinary algorithm including MMR immunohistochemistry, MLH1 promoter methylation studies, and MMR germline testing (figure 1).

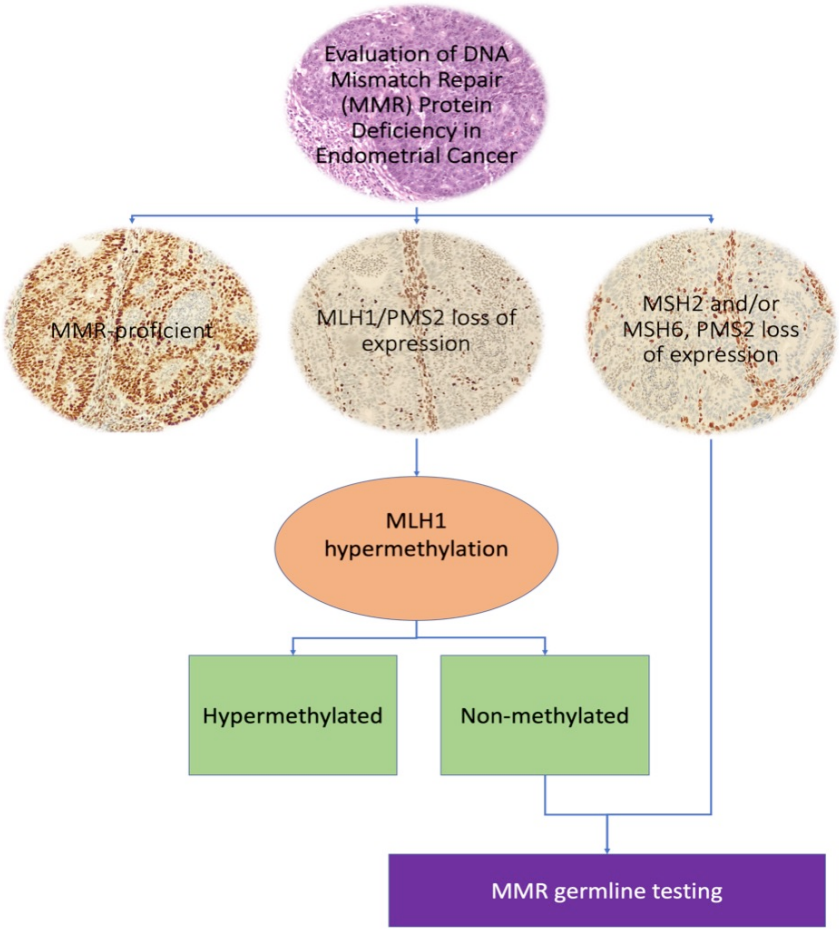

Figure 1. Flow chart of diagnosis of Lynch syndrome in endometrial cancers.

Women who inherit mutations in the *BRCA* genes or the *PTEN* gene (Cowden syndrome) may also be at an increased risk of developing endometrial cancer.

Cowden syndrome is an autosomal dominant disorder frequently associated with germ line mutations in the *PTEN* tumor suppressor gene located on chromosome 10. It is characterized by several hamartomas and malignancies that develop in multiple organs with increased risk for the breast and, to a lesser extent, thyroid, kidney, colon, and endometrium. The lifetime risk of endometrial carcinoma in women with Cowden syndrome is estimated to be between 5% and 10% compared to 2.6% in the general population.

Endometrial carcinoma occurs in up to 28% of Cowden syndrome patients. Most tumors are low-grade endometrioid carcinomas with loss of PTEN by immunohistochemistry, the latter which is also commonly seen in sporadic cases.

Histopathologic Classification of Endometrial Carcinoma

Endometrial adenocarcinomas are a heterogeneous group of tumors derived from endometrial glandular epithelial cells. Endometrial cancers can be histologically classified according to the World Health Organization [10] (see table 1).

Table 1. Histological subtypes of endometrial carcinoma

Histological types	Frequency
Endometrioid carcinoma	75-80%
Non-endometrioid carcinoma	20-25%
Serous carcinoma	5-10%
Clear cell carcinoma	1-6%
Mixed carcinoma	5-10%
Undifferentiated/Dedifferentiated carcinoma	1-2%
Carcinosarcoma	5%
Others	<1%

Endometrioid carcinoma

Endometrioid endometrial carcinoma (EEC) is the most common subtype, accounting for 75- 80% of endometrial cancer that usually develop in a background of endometrial hyperplasia. EEC is a malignant epithelial neoplasm displaying varying proportions of glandular, papillary, and solid architecture, with the neoplastic cells showing endometrioid differentiation [10]. The term “endometrioid” derives from the tumor’s predominant glandular pattern, which resembles proliferative- phase endometrium.

Conventional EEC is identified by complex, branching glandular or villoglandular architecture composed of back to back glands with no intervening stroma. These (villo)glandular structures typically show a smooth luminal outline and are lined by stratified or pseudostratified columnar cells with usually only modest amounts of pale to lightly eosinophilic cytoplasm with rounded nuclei. Nuclear pleomorphism is variable but is usually only mild to moderate with inconspicuous nucleoli, except in high-grade EEC. The mitotic count is highly variable. Squamous differentiation is frequent (occurring in 10–25% of cases). Association with the precursor lesion (atypical hyperplasia / endometrioid intraepithelial neoplasia - EIN) may be seen. Histologic variants, which are not associated with different prognosis, include secretory patterns (resembling those of early secretory endometrium, either focal or diffuse, mimicking clear cell carcinoma), small non-villous papillae, microglandular pattern, spindle cell pattern, sertoliform pattern, and sex cord–like formations and hyalinization. Mucinous pattern may be present in varying degrees and may predominate.

Immunohistochemical and molecular findings

ECCs have molecular alterations that differ from non-endometrioid carcinomas, including mutations in *PTEN* (leading to loss of PTEN staining in 75% of tumors), *KRAS*, *CTNNB1* (leading to β-catenin nuclear expression), *PIK3CA, ARID1A*. Defects in DNA MMR leading to microsatellite instability occur in about a third of tumors. *TP53* mutation/abnormal p53 expression is reported in 2–5% of low-grade and 20% of high-grade EEC. Low-grade EEC usually shows diffuse strong immunoreactivity for ER/PR and Vimentin, and patchy positivity for p16.

Serous carcinoma

Serous carcinomas (SC) represent approximately 10% of all endometrial carcinomas but account for as many as 40% of endometrial cancer–related deaths. SC is a carcinoma with diffuse, marked nuclear

pleomorphism, typically exhibiting papillary and/or glandular growth patterns [10]. SC typically arises in a background of atrophic endometrium or in an endometrial polyp. Typical microscopic features include complex papillary and/or glandular architectural pattern. The papillae are constituited by broad, thick fibrovascular cores, but occasionally thin to delicate cores, covered by a stratified epithelium with a prominent and tufting or budding pattern, with many groups of detached cells lying free between the papillae. The tumor cells are often hobnail and contain abundant granular eosinophilic or clear cytoplasm. The nuclei are high grade, with marked pleomorphism and large macronucleoli along with occasional bizarre and hyperchromatic giant nuclei. Mitotic figures are numerous and abnormal mitoses are easily identified. Psammoma bodies are sometimes seen. Deep myometrial invasion and lymph vascular space invasion are often evident. Carcinoma replacing the native surface and glandular epithelium without associated invasion (serous endometrial intraepithelial carcinoma - SEIC) may be present adjacent to serous carcinoma or identified in the absence of invasive disease. In the absence of demonstrable invasion, the intraepithelial lesions can shed malignant cells and metastasize to extrauterine sites and they should be considered as potentially metastatic.

Immunohistochemical and molecular findings

TP53 mutation is the molecular hallmark of serous carcinoma and is reflected by a mutation-pattern p53 immunostaining. Additional common genetic alterations involve *PIK3CA*, *PP2R1A*, and *FBXW7*. *ERBB2* (*HER2*) amplification is present in 30% of cases, frequently heterogeneously distributed. Diffuse expression of p16, IMP3, and HMGA2 are typical. ER/PR staining is variable. Unlike in grade 3 endometrioid carcinoma, aberrant staining for PTEN, β-catenin, ARID1A and mismatch repair proteins is very uncommon.

Clear cell carcinoma

Clear cell carcinoma (CCC) account for 1–6% of endometrial carcinomas and occur at an older age than endometrioid adenocarcinoma. CCC is a carcinoma demonstrating papillary, tubulocystic, and/or solid architectural patterns and variably pleomorphic polygonal, cuboidal, flat, or hobnail cells with clear or eosinophilic cytoplasm [10].

The major architectural patterns (tubulocystic, papillary, and solid) are frequently admixed. Papillae are small, regular and frequently hyalinized. Tumor cells are polygonal to cuboidal and flattened with clear to eosinophilic cytoplasm and may have hobnail morphology. Nuclear pleomorphism is variable, but at least focal moderate to severe atypia is typically present. Mitotic activity is variable, but most tumors display < 6 mitoses/10 high power fields (HPF). Eosinophilic extracellular globules or hyaline bodies are also a characteristic feature, present in approximately two thirds of these tumors. Similar to serous carcinoma, these tumors arise in polyps or atrophic endometrium.

Immunohistochemical and molecular findings

Immunohistochemically, CCC are typically ER/ PR negative and positive for HNF1β, Napsin A, and AMACR (P504S); 22–72% of cases display mutation-pattern p53 staining. Recurrent somatic mutations include mutations in *TP53*, *PPP2R1A*, *PIK3CA, PIK3R1, KRAS, ARID1A*, and *SPOP*. High microsatellite instability is reported in 11–14% of cases and MMR protein deficiency is variable (0–33%).

Mixed endometrial carcinomas

Mixed endometrial carcinomas are rare; mixed endometrioid and serous carcinomas account for about 5-10% of endometrial carcinomas. Mixed carcinoma is a carcinoma composed of two or more discrete histological types of endometrial carcinoma, where at least one component is either serous or clear cell

[10]. At least two spatially distinct histotypes of endometrial carcinoma must be identified by histology and immunohistochemistry.

Undifferentiated and dedifferentiated carcinomas

Undifferentiated endometrial carcinoma (UC) is a rare, highly aggressive, and under-recognized subtype of endometrial cancer. Endometrial undifferentiated carcinoma is a malignant epithelial neoplasm with no overt cell lineage differentiation. Dedifferentiated carcinoma (DEDC) is composed of an undifferentiated carcinoma and a differentiated component (typically of FIGO grade 1 or 2 endometrioid carcinoma) [10].

UC is composed of predominant dyscohesive monotonous medium to large sized cells, with patternless growth pattern or solid sheet-like growth with total absence of nests, papillae, glands or trabeculae. UC may resemble lymphoma, plasmacytoma, high-grade endometrial stromal sarcoma, or small cell carcinoma. No gland formation is present; however, abrupt keratinization can be seen. Tumor cells exhibit vesicular nuclei with prominent eosinophilic nucleoli, occasional hyperchromasia, marked nuclear pleomorphism and multinucleation. Occasionally, tumors can exhibit rhabdoid morphology. Large areas of geographic necrosis with viable perivascular tumor cells are usually seen. Mitoses and apoptotic figures are numerous. Although the stroma is generally unapparent, some tumors have a myxoid matrix. Prominent tumor infiltrating lymphocytes are usually present.

Dedifferentiated carcinoma is characterized by abrupt interface between the undifferentiated component and a second component of differentiated carcinoma, which is most frequently a FIGO grade 1 or 2 endometrioid carcinoma.

Immunohistochemical and molecular findings

UC/DEDC display evidence of epithelial differentiation in only occasional neoplastic cells, typically with very focal but intense and often perinuclear dot-like staining for EMA and keratin; diffuse strong staining with pancytokeratin should not be present. Neoplastic cells express vimentin but are negative for ER/PR and E-cadherin. PAX8 is usually negative. Chromogranin and/or synaptophysin staining can be identified in a minority of tumor cells, usually < 10%. Loss of SMARCA4 (BRG1) expression is present in approximately one third of UC. Microsatellite instability/MMR deficiency is reported in half to two thirds of dedifferentiated and half of undifferentiated carcinomas. UC/DEDC carcinomas can also show *POLE* and *TP53* mutations.

Carcinosarcoma

Carcinosarcomas (CS) account for 5% of all uterine malignancies and represent a highly aggressive tumor. Carcinosarcoma is a biphasic tumor composed of high-grade carcinomatous and sarcomatous components [10].

Tumors consist of an admixture of carcinomatous and sarcomatous components, which is typically sharply juxtaposed. The epithelial component most often shows endometrioid or serous differentiation, but clear cell and undifferentiated carcinoma may be encountered. The mesenchymal component most commonly consists of high-grade sarcoma NOS (not otherwise specified) , but heterologous elements (including rhabdomyosarcoma, chondrosarcoma, and rarely osteosarcoma) may be seen. Deep myometrial and lymph vascular invasion are usually present.

Immunohistochemical and molecular findings

Epithelial and mesenchymal components have similar genetic alterations. It is now known that the sarcoma is derived from the carcinoma as a result of transdifferentiation (epithelial–mesenchymal transition) during tumor evolution. Most cases are characterized by *TP5*3 mutations (90%), similar to endometrial serous carcinoma.

FIGO grade

The International Federation of Obstetricians and Gynecologists (FIGO) provides a 3-tiered system for grading endometrioid endometrial carcinoma based on the degree of glandular differentiation and cytologic atypia [11]. Grade 1 tumors exhibit ≤5% solid non-glandular, non-squamous growth; grade 2 tumors from 6% to 50%; and grade 3 tumors >50%. The presence of severe cytological atypia in the majority of cells (> 50%) increases the grade by one level. The non-endometrioid histotypes (i.e. serous, clear cell and undifferentiated/dedifferentiated carcinomas) – regardless of either growth pattern or cytologic atypia – are classified as grade 3. This grading system proved to have interobserver variability and 2020 WHO classification recommends moving toward a binary scheme to grade endometrial endometrioid carcinomas by FIGO grades 1 and 2 tumors as “low grade” and grade 3 tumors as “high grade” [10].

FIGO stage

The 2 systems used for staging endometrial cancer, the FIGO (International Federation of Gynecology and Obstetrics) system and the American Joint Committee on Cancer TNM staging system are basically the same [12, 13]. FIGO staging system provides four stages based on the extent of tumor growth and several risk factors (such as depth of the myometrial invasion, extension into the cervical canal, pelvic node metastases, aortic node metastases, adnexal metastases, involvement of uterine serosa and positive

peritoneal cytology). Accurate pathological assessment of depth of myometrial invasion and cervical stromal involvement is essential for FIGO staging. Tumors confined to the uterine corpus with less than 50% myometrial invasion are stage IA, whereas stage IB tumors are those with greater than 50% myometrial invasion. In stage II tumors infiltrate cervical stroma (see table 2).

Table 2. FIGO staging system for endometrial cancer

Stage I	Tumor confined to the corpus uteri
	IA No or less than half myometrial invasion
	IB Invasion equal to or more than half of the myometrium
Stage II	Tumor invades the cervical stroma, but does not extend beyond the uterus
Stage III	Local and/or regional spread of tumor
	IIIA Tumor invades the serosa of the corpus uteri and/or adnexas
	IIIB Vaginal and/or parametrial involvement
	IIIC1 Positive pelvic lymph nodes
	IIIC2 Positive para-aortic lymph nodes with or without positive pelvic lymph nodes
Stage IV	Tumor invades bladder and/or bowel mucosa and/or distant metastases
	IVA Tumor invades bladder and/or bowel mucosa
	IVB Distant metastases, incl. intra-abdominal metastases and/or inguinal lymph nodes

Therapy

Surgery

The diagnosis of endometrial cancer will depend on the preoperative histopathological assessment. The standard approach for the management of endometrial cancer is hysterectomy and bilateral salpingo-oophorectomy with or without lymphadenectomy (see table 3). The procedure can be performed by laparotomy or laparoscopy, but recently the second one is highly preferred as less invasive, safer and cost-effective. Lymphadenectomy is an integral part of the comprehensive surgical staging of endometrial cancer. However, the role of lymphadenectomy in early endometrial cancer is unclear and controversy

remains regarding the indications for, the anatomic extent of, and the therapeutic value of lymphadenectomy in the management of the disease. ESMO-ESGO-ESTRO guidelines recommend complete surgical staging in the case of high-grade carcinomas [14].

In young women a conservative management approach could be considered in patients with a histological diagnosis of grade 1 endometrial carcinoma (or premalignant disease such as EIN). The optimal method to obtain these histologic characteristics is dilatation and curettage; this procedure is superior to pipelle biopsy in terms of accuracy of the tumor grade [14].

Table 3. ESMO endometrial cancer surgical management algorithms based on preoperative assessment*.

Clinical Stage	Risk group	Surgery	Lymphadenectomy†
Clinical Stage I	Low risk: clinical stage IA, G1/2, endometrioid type	Total hysterectomy and bilateral salpingo-oopho-rectomy without vaginal cuff‡§	Not recommended
	Intermediate risk: clinical stage IA, G3, endometrioid type clinical stage IB, G1/2, endometrioid type	Total hysterectomy and bilateral salpingo-oopho-rectomy without vaginal cuff	Can be considered for staging. SLND is an option
	High risk: clinical stage IB, G3, endometrioid type all stages with non-endometrioid type All stages with non-endometrioid type	Total hysterectomy and bilateral salpingo-oopho-rectomy without vaginal cuff	Recommended
Clinical Stage II		Total hysterectomy and bilateral salpingooopho-rectomy; modified (type B) or type A radical hysterectomy to be considered if required for obtaining free margins	Recommended to guide staging and adjuvant therapy
Clinical Stages III – IV		Good PS: where feasible, complete macroscopic cytoreduction (including resection of metastases) Impaired PS or unresec-table disease: multimodal-ity treatment to be considered (including cases when surgery may significantly impair vaginal function)	Recommended as part of comprehensive stag-ing

***Mandatory and additional assessments as below: mandatory assessments: family history, chest x-ray (when abdominal CT is performed, thoracic assessment can replace chest x-ray), clinical and gynecologic assessment (including inventory of comorbidities, and geriatric assessment, if appropriate), transvaginal ultrasound, complete pathology assessment (histotype and grade) by endometrial biopsy/curettage +/− hysteroscopy if needed. Additional assessments: abdominal CT (to investigate extrapelvic disease), contrast enhanced MRI (to assess cervical involvement and/or myometrial invasion in apparent stage I EC (MRI to assess myometrial invasion in apparent stage I EC should only be undertaken in institutions where the indication for LND is tailored according to risk groups).**

†Lymphadenectomy to include systematic removal of pelvic and paraaortic nodes up to the level of the renal veins.

‡Ovarian preservation can be considered in women <45-yr old with <50% myometrial invasion, no obvious extrauterine disease and no family history of ovarian cancer risk.

§Patients with AH/EIN or G1 EEC requesting fertility-preserving therapy must: be referred to specialized centers; undergo D&C with or without hysteroscopy; have AH/EIN or G1 EEC confirmed by a specialist gynecologic pathologist; undergo pelvic MRI to exclude overt myometrial invasion and adnexal involvement; be fully informed that fertility-sparing treatment is a nonstandard treatment; be willing to accept close follow-up.

For patient undergoing fertility-preserving therapy, medroxyprogesterone acetate (MPA) or megestrol acetate (MA) is recommended; progestinloaded IUD is also an option. After completion of childbearing, hysterectomy, and salpingo-oophorectomy is recommended.

CT indicates computed tomography; ESMO, European Society for Medical Oncology; MRI, magnetic resonance imaging; SLND, sentinel lymph node dissection.

Adjuvant therapy

The majority of patients with endometrial cancer have a low risk of recurrence and are managed by surgery alone. In order to identify patients at risk of recurrence who may benefit from adjuvant therapy, ESMO 2016 risk classification defined four groups based on the combination of clinicopathological factors: age, FIGO stage, depth of myometrial invasion, tumor differentiation grade, tumor type (endometrioid versus serous and clear cell) and lymph vascular space invasion (see table 4). The risk of disease recurrence is classified in low-, intermediate-, high-intermediate and high-risk [14]. Patients in the first group have a good prognosis and do not benefit from adjuvant therapy, which is instead suggested for the remaining 3 groups. The therapy consists of radiation or chemotherapy (that can be combined particularly for patients with a high risk for recurrence), and the treatment can be different depending on local practices. Vaginal brachytherapy is an option for patients with an intermediate risk, its efficacy in the prevention of the local recurrences has been proved, but it has less toxicity than external radiotherapy. Hormonal therapy can be used in a postoperative adjuvant regimen, but its survival benefits are still under study. Although the efficacy of adjuvant therapy for patients with high-risk features remains an area of controversy, external beam radiotherapy is currently recommended, and adjuvant platinum-based chemotherapy can be considered for stage III or IV, and non-endometrioid cancers. (see table 4).

Table 4. ESMO endometrial cancer adjuvant treatment algorithm based on final histotype and postsurgical staging according to FIGO 2009 system.

ESMO 2016 RISK GROUP	NODAL STATUS	ADJUVANT TREATMENT
Low risk EEC: **Stage I grades 1–2, <50% myometrial invasion,** **LVSI negative**	NA	No adjuvant treatment
Intermediate risk EEC: **Stage I, grades 1–2, ≥ 50% myometrial invasion,** **LVSI negative**	NA	Adjuvant brachytherapy No adjuvant therapy is an option, especially for patients <60-yr old
High-intermediate risk EEC: **Stage I, grade 3, <50% myometrial invasion, regardless of LVSI status** **Stage I, grades 1–2, LVSI unequivocally positive; regardless of depth of myometrial invasion**	Surgical nodal staging performed, node negative	Adjuvant brachytherapy No adjuvant therapy is an option
High-risk EEC: **Stage I, grade 3, ≥ 50% myometrial invasion, regardless of LVSI status**	No surgical nodal staging Performed Surgical nodal staging performed, node negative No surgical nodal staging performed	Adjuvant brachytherapy for G3 and LVSI negative Adjuvant EBRT for LVSI unequivocally positive Adjuvant EBRT with limited fields Adjuvant brachytherapy is an alternative option Adjuvant EBRT Adjuvant chemotherapy (combined and/or sequential) can be considered (greater evidence to support combined chemotherapy plus EBRT than either individual modality alone)
High-risk EEC: Stage II	Surgical nodal staging performed, node negative No surgical nodal staging performed	Adjuvant vaginal brachytherapy for G1-2 LVSI negative Adjuvant limited field EBRT for G3 or LVSI unequivocally positive; consider brachytherapy boost Adjuvant EBRT, consider brachytherapy boost Adjuvant chemotherapy for G3 or LVSI unequivocally positive (combined and/or sequential) should be considered
High-risk EEC: Stage III, no residual disease		Chemotherapy plus EBRT to be considered for IIIA, IIIB and IIIC1 Chemotherapy plus enhanced field EBRT to be considered for IIIC2
High risk, non-endometrioid cancer (serous or clear-cell or undifferentiated carcinoma or carcinosarcoma)		Serous and clear cell after comprehensive staging: Chemotherapy (clinical trials encouraged) Stage IA, LVSI negative: Vaginal brachytherapy Stage ≥ IB: EBRT plus chemotherapy especially if node positive Carcinosarcoma and undifferentiated tumors: Chemotherapy Consider EBRT (clinical trials encouraged)

EBRT indicates external beam radiotherapy; EEC, endometrioid endometrial carcinoma; ESMO, European Society for Medical Oncology; FIGO, International Federation of Gynecology and Obstetrics; LVSI, lymphovascular space invasion; NA, not applicable.

Follow-up and recurrent disease

The recurrence of endometrial cancer is estimated to be >30% for patient with high-risk features, while it dropped to 15-10% for intermediate-risk group, and 5-10% for low-risk group. In presence of adjuvant radiotherapy, a lower number of vaginal or pelvic recurrences has been observed, but not impact can be seen on distant metastasis or overall survival. The follow up typically involves a period of 3-5 years of surveillance. Most of the recurrences are diagnosed in the first three years, and an early stage detection will result in a higher salvage rate. Vaginal recurrence is more frequent if adjuvant radiotherapy was not performed. Pelvic and para-aortic nodal recurrences, peritoneal and lung metastases are relatively commonly observed in patients of intermediate and high-risk groups.

Molecular characterization of endometrial cancer

The Cancer Genome Atlas (TCGA) classification

In 2013, The Cancer Genome Atlas (TCGA) collaborative project has reported an integrated genomic, transcriptomic and proteomic characterization of endometrial cancers. TCGA analysis identified four distinct prognostic EC groups based on molecular alterations: (i) the ultramutated subtype that encompassed *POLE* exonuclease domain mutated (*POLE*) cases (excellent prognosis); (ii) the hypermutated subtype, characterized by microsatellite instability/MisMatch Repair deficiency (MMRd) (intermediate prognosis); (iii) the “copy-number high subtype”, with *TP53* mutations/p53 abnormal (p53abn) (poor prognosis); (iv) the copy-number low subtype, also known as No Specific Molecular Profile - NSMP (intermediate prognosis) [15]. *POLE*-mutant endometrial tumors are characterized by hotspot mutations in exonuclease domain of *POLE* (subunit of DNA polymerase epsilon) and very high mutation rates,

increased frequency of C>A transversions, few copy number alterations, mutations in *PTEN*, *PIK3R1*, *PIK3CA*, *FBXW7*, and *KRAS*, and favorable outcome. Microsatellite unstable endometrial cancers are characterized by *MLH1* promoter hypermethylation, high mutation rates, few copy-number alterations and *PIK3CA* and *PTEN* mutations. The "copy-number high" group consists primarily of serous and one-fourth of high-grade endometrioid endometrial cancers with low mutational rates, recurrent *TP53*, *FBXW7*, and *PPP2R1A* mutations and poor outcome. The "copy-number low" group include microsatellite stable endometrial cancers with low mutational rates, characterized by frequent *CTNNB1* mutations and chromosome 1q amplification. In view of these findings, Bokhman's dualistic model of endometrial cancer has been even further extended by the integration of molecular features both for prognostic and therapeutic purposes.

Translation of the TCGA molecular groups into the clinical practice is an emerging challenge. Two groups independently proposed and validated the same surrogate markers (*POLE* mutation, microsatellite instability/MMR deficiency, and p53 mutation/alteration) to identify TCGA groups in routine clinical practice [16-18]. The ProMisE (ProactiveMolecular Risk Classifier for Endometrial Cancer) algorithm applies *POLE* mutation, p53 and MMR protein expression analyses to sequentially assign first the MMR deficient group, then *POLE* mutant, and finally aberrant p53 cases; the remaining tumors are categorized as p53 normal [17, 18]. Similarly, the TransPORTEC initiative has identified four prognostic groups, identifying first *POLE* proofreading mutant tumors, then subsequently MMRd tumors, p53-mutant tumors, and a group with no specific molecular profile (NSMP) [16]. In both algorithms, prognostic signatures emerged by stratifying endometrial cancer tumors according to these specific molecular criteria.

CTNNB1 mutations in endometrial carcinoma

Some studies evaluated the potential prognostic impact of *CTNNB1* mutations in low-grade early-stage EC showing a significantly worse disease-freesurvival [19, 20]. The prognostic significance of *CTNNB1*

mutations within NSMP EC may qualify *CTNNB1* mutant EC as a separate biomolecular entity representing the fifth molecular EC group (after exclusion of cases belonging to the *POLE*, MMRd and p53 abn classes).

ARID1A mutation in endometrial carcinoma

Among the molecular alterations investigated in EC stand out those affecting proteins of the switch/sucrose non-fermenting chromatin remodeling complex (SWI/SNF), in particular SMARCA4 (BRG-1), SMARCB1 (INI-1) and ARID1A/B. The SWI/SNF complex performs essential functions that permit gene expression, altering the structure of nucleosomes and allowing direct access to genes for their transcription. Mutations affecting the subunits that make up this complex may result in the alteration of several chromatin-related processes, including DNA repair, DNA synthesis, mitosis, and genomic instability. The *AT-rich interactive domain 1A* (*ARID1A*) gene encodes the protein BAF250a, which is a key component of the multi-protein SWI/SNF chromatin remodeling complex [21]. Mutations in *ARID1A* occur across the entire gene and are generally inactivating (frameshift or truncation). These mutations result in loss of ARID1A protein, which is detectable by immunohistochemistry, consistent with a loss of function mechanism of oncogenesis. Loss of ARID1A expression determines a complex set of SWI/SNF functional alterations: (i) defects in the enhancer-mediated gene regulation of cell cycle checkpoint activation in response to DNA damage [22]; (ii) alteration in the expression of genes regulated by nuclear hormonal receptors; and (iii) a deregulation of the developmental gene expression while maintaining cell self-renewal, survival and proliferative capacity [23].

ARID1A is mutated in approximately 30-40% of both low- and high-grade endometrioid ECs, but not in serous endometrial carcinomas [24-26]. Some studies demonstrated that *ARID1A* mutation is associated with mismatch repair deficiency and normal p53 expression [27, 28]. Furthermore, loss of ARID1A in complex atypical hyperplasia is associated with malignant transformation and concurrent EC [29], and promotes epithelial-to-mesenchymal transition (EMT) and myometrial invasion [30].

All these observations about the role of ARID1A in regulating enhancer-mediated gene expression, in tumor suppression and in the regulation of differentiation programs, have encouraged us to investigate the significance of ARID1A alterations in refining the molecular classification of EC.

Thesis outline

Histopathological evaluation, including subtyping and grading, is the current cornerstone for endometrial cancer (EC) classification. EC prognosis is traditionally defined by a combination of clinical and histopathologic criteria (e.g. histotype, grade, lymph vascular invasion, stage) that are also used to tailor surgery and to select patients for adjuvant therapy. Unfortunately, the assessment of histologic parameters is poorly reproducible and conventional clinicopathologic features do not reliably predict either the patient's response to the available treatment or the definition of personalized forms of therapy [31]. The Cancer Genome Atlas (TCGA) endometrial collaborative project identified four distinct prognostic EC groups based on molecular alterations: (i) *POLE* ultramutated (*POLE*), (ii) mismatch repair-deficient (MMRd), (iii) p53 mutant (p53abn) and (iv) those EC lacking any of these alterations, referred to as NSMP (No Specific Molecular Profile) [15]. Although the four TCGA molecular groups appear to have different prognosis, it has become clear that the NSMP tumors (the majority of endometrial cancer cases) represent a heterogeneous group of carcinomas with variable molecular alterations and divergent clinical outcomes. Further investigations are needed to refine the biology and prognosis of the NSMP group.

The aims of this thesis are:

1. to evaluate the prognostic stratification based on conventional clinicopathologic criteria according to ESMO 2016 risk group criteria in a single center, population-based series of EC;

2. to investigate the feasibility and the prognostic impact of the novel surrogate TCGA molecular classification of endometrial carcinoma;

3. to correlate EC histopathologic characteristics with molecular subtypes;

4. to define the relevance of *ARID1A* and *CTNNB1* mutations and their predictive-prognostic weight with particular reference to the NSMP group;

5. to integrate ESMO 2016 risk stratification criteria with molecular subtyping;

6. to propose a workable and useful algorithm in routine clinical practice for improving risk stratification and patient management.

Materials and Methods

Study cohort and clinicopathologic data

The study was approved by the local research ethics committee CE-AVEC (Comitato Etico—Area Vasta Emilia Centro, registration n. 27/2019/Sper/AOUBo). All patients signed an informed consent permitting the use of their normal as well as neoplastic tissue and the data necessary for the study. All patients underwent surgical resection with staging at the Gynecologic Oncology Unit of "Policlinico di S.Orsola", University of Bologna (Bologna, Italy) [32]. Formalin-fixed paraffin-embedded (FFPE) tissue blocks containing representative tumor samples were selected from 125 consecutive primary endometrial carcinomas in the files of the Pathology Unit of Policlinico di S. Orsola", University of Bologna (Bologna, Italy). The selected blocks were used to assess histopathologic parameters, for immunohistochemical and molecular analyses. In order to minimize biases due to tumor heterogeneity we used whole-tissue sections from surgical resection rather than tissue microarrays or small biopsy samples for histologic, immunohistochemical and molecular analyses. The histology slides and all histopathologic parameters were thoroughly reviewed by two expert pathologists (DS, ADL). Clinical data were obtained from clinical, surgical and pathologic records reported in a comprehensive clinicopathologic database included: age at diagnosis, Body Mass Index (BMI), International Federation of Gynecology and Obstetrics (FIGO) stage determined using surgical reports, ESMO 2016 risk stratification group, type of surgery, peri-operative complications, imaging studies, pathology reports, and clinical findings including follow-up data.

- Tumors were classified according to standard *histopathologic criteria* following the World Health Organization classification of tumors [33] and graded using standard FIGO criteria [34].

- The *depth of myometrial invasion* was recorded in all cases as a percentage of myometrial thickness.
- The *pattern of myometrial invasion* was reported, specifying whether microcystic, elongated and fragmented (*MELF*) [35] and/or as single invasive cells or small groups of cells (*tumor budding*) [36]. Characteristics of the MELF pattern include the presence of invasive small dilated glands lined by cuboidal or flattened cells with eosinophilic cytoplasm and with slit-like appearance. This invasive pattern typically has a myxoid to granulation-like reaction in the surrounding myometrium. Tumor budding is defined as invasive single/small group of cells without formation of defined structures frequently lying in an edematous or myxoid background.
- *Lymph vascular space invasion* (LVSI) is defined by the presence of tumor fragments within endothelial-lined vascular/lymphatic spaces outside the immediate invasive border. Intratumoral LVSI foci were not considered. A semi-quantitative *three- tiered* scoring system was applied: no LVSI; focal (a single focus of LVSI recognized around the tumor); substantial (diffuse or multifocal LVSI around the tumor) [37, 38].
- The presence of *extensive tumor necrosis* was reported; necrosis only within glands or at the tumor's surface was not scored.
- *Tumor heterogeneity* were reported when a tumor had two or more clearly separate morphological patterns, and each constituting at least 10% of the tumor [39].
- *Tumor infiltrating lymphocytes* were assessed considering intraepithelial tumor infiltrating lymphocytes (*iTILs*; lymphocytes located within the tumor epithelium) and stromal tumor infiltrating lymphocytes (*sTILs*; lymphocytes in the stroma immediately adjacent to the tumor epithelium). The number of intraepithelial lymphocytes was counted in ten high-power fields (HPF, 40X objective) with the highest density of TILs. The cut-

off of 40 lymphocytes per 10 HPF was used to define a high iTIL score [39, 40]. sTILs counting was evaluated at X400 magnification field from the invasive border and performed according to the semi-quantitative method of Shia: sTILs absent/mild and sTILs moderate/high [39, 40].

- The *mitotic index* was expressed as the number of mitoses per 10 high-power fields (40X).

Immunohistochemistry

The details of the immunohistochemistry (IHC) methods to assess p53, PTEN, ARID1A, β-Catenin, MLH1, PMS2, MSH2, MSH6, and Ki67 are described in supplemental table 1. Slides were evaluated by two observers (ADL, CC) without knowledge of the patient's characteristics and outcome.

Immunohistochemical assessment and evaluation of p53 expression: p53 was considered abnormal/mutant-like (p53abn) if more than 50% of the tumor cells showed strong positive nuclear staining, or when areas (subclones) consisting of > or =50% positive tumor cells were present, or when no nuclear p53 staining was evident in the entire tumor. In addition to nuclear overexpression of p53 and complete absence of nuclear p53 staining (null pattern) a third mutant pattern showing strong cytoplasmic overexpression has been considered [41].

Immunohistochemical assessment and evaluation of PTEN expression: PTEN was considered negative if no cytoplasmic/nuclear immunostain was identified in the neoplastic cells; cases were considered positive if uniform or heterogeneous staining was identified in the neoplastic cells [42].

Immunohistochemical assessment and evaluation of ARID1A expression: ARID1A nuclear staining was scored as follows: negative "loss of expression", "positive" (weak or strong) or as "clonal loss" [28]. In the final analysis, "clonal loss" was reclassified as "loss of expression"as this pattern corresponded to subclonal *ARID1A* mutations.

Immunohistochemical assessment and evaluation of β-catenin expression: β-catenin was classified as "normal" when only membranous/cytoplasmic staining was present or "abnormal" when there was nuclear immunoreactivity. Weak nuclear staining associated with cytoplasmic/membranous expression in occasional cells was considered "normal" because the same pattern of immunoreactivity was observed in normal endometrium [43, 44].

Immunohistochemical assessment and evaluation of MMR protein expression: MLH1, PMS2, MSH2, and MSH6 were scored negative if no nuclear immunostaining was present. Cases were considered mismatch repair deficient (MMRd) if one of the four proteins was absent or if MLH1/PMS2 or MSH2/MSH6 were negative.

Immunohistochemical assessment and evaluation of Ki67 proliferation index: the evaluation of the proliferative index (Ki67) in the neoplastic population was carried out quantitatively using image analysis with the IMAGE ProPlus 5.1 software (Media Cybernetics Inc.) in at least forty 200x fields, and expressed as the ratio (%) between the positive neoplastic cells and the total neoplastic cells.

DNA extraction and Next Generation Sequencing

DNA was extracted from FFPE tissue starting from two to four 10-µm-thick sections, according to the amount of neoplastic tissue present in the paraffin block. The areas of interest were marked on the control Hematoxylin and Eosin (H&E) stained slide and manually dissected under microscopic guidance using a sterile blade. DNA was extracted using the Quick Extract Kit (Epicentre, Madison, WI, USA) and quantified using the "Qubit" fluorometer (Thermo Fisher Scientific, MA, USA). Samples were analyzed using a customized panel of genomic regions and sequenced using the Gene Studio S5 sequencer (ThermoFisher Scientific, Waltham, MA, United States), according to the manufacturer's instruction (ThermoFisher Scientific, Waltham, MA, United States) as previously published [45]. Template preparation was performed using the Chef Machine instrument (ThermoFisher Scientific,

Waltham, MA, United States) and then sequenced using an Ion 530 chip. The panel included a total of 169 amplicons within the following gene regions: *ARID1A* (all CDS region), *BRAF* (exon 15), *cKIT* (exons 8, 9, 11, 13, 17), *CTNNB1* (exons 3, 7, 8), *HRAS* (exons 2-4), *KRAS* (exons 2-4), *NRAS* (exons 2-4), *PIK3CA* (exons 10, 21), *POLE* (exons 9-14), and *TP53* (exons 4-9).

Only nucleotide variations in at least 5% of the total number of reads analyzed were considered for mutational call. The sequences obtained were analyzed using the Ion Reporter Software (version 5.10.5, ThermoFisher Scientific, Waltham, MA, United States) and the Integrative Genomics Viewer 2.5 (IGV) tool (http://software.broadinstitute.org/software/igv/).

Methylation specific PCR

Tumors with loss of MLH1 protein expression were selected for further testing for methylation status of the 5' regulatory region of MLH1, using methylation-specific PCR, with previously reported primers [46].

Assignation of carcinomas to surrogate TCGA molecular groups and NSMP sub-groups

The steps in immuno-molecular classification are illustrated in figure 2. First, all cases were assessed for pathogenic *POLE* mutations to identify "ultramutated" group tumors (*POLE*). Diagnostic interpretation of *POLE* mutations was based according to reported guidelines [47]. The next assessment was the immunohistochemical determination of mismatch repair (MMR) proteins expression to identify MMR deficient (MMRd) tumors and to assign tumors to the TCGA "hypermutated" group (in absence of *POLE* mutation). Subsequently, tumors were evaluated by IHC for p53 to detect p53 abnormal (p53abn) tumors corresponding to the "copy number-high/serous-like" TCGA group. Tumors exhibiting normal p53 and MMR expression by IHC with no *POLE* mutations, were defined as "No specific molecular profile"

(NSMP) tumors and correspond to the "copy number-low" subgroup in the TCGA. This latter group was split into two subgroups according to *CTNNB1* mutations/ β-catenin abnormal expression: β-catenin abnormal (β-CATabn) and β-catenin wild-type (NSMP). Each of these subgroups was further stratified according to *ARID1A* mutations/ ARID1A loss of expression (β-CATabn/β-CATabn_A, NSMP/NSMP_A).

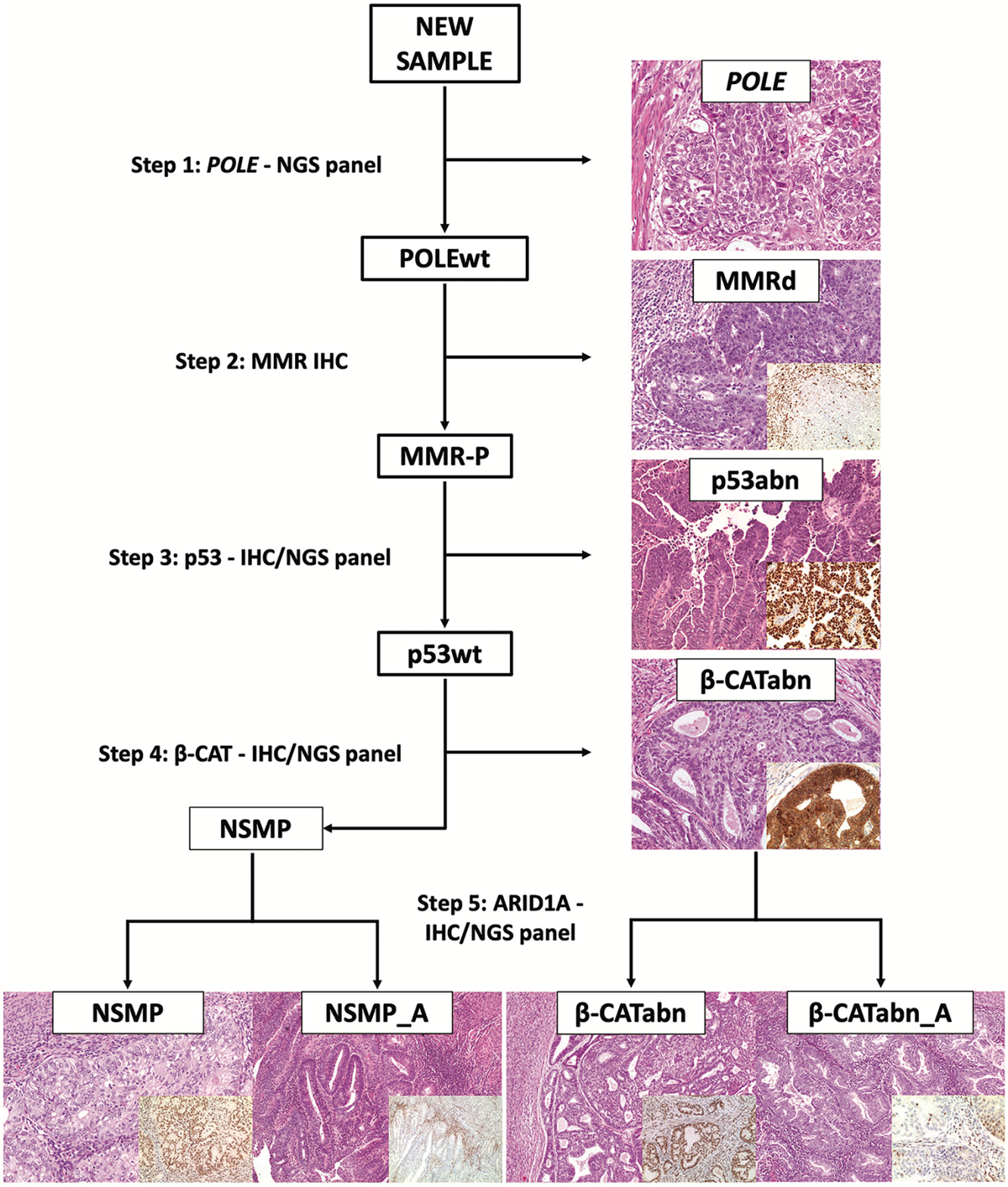

Figure 2. Diagnostic algorithm for the "immuno-molecular" classification of endometrial carcinoma.

Statistics

Summary statistics are reported as numbers (percentages) or mean ± standard deviation.

Crude comparisons between groups were performed using Fisher's exact test, chi-squared test, Kruskal–Wallis test, t-test and Mann–Whitney test, when appropriate. We used the Kaplan-Meier estimator to display disease-free survival and overall survival following surgery; the equality of survivor functions was assessed using the log-rank test. All deaths from disease were considered an event; all recurrences (local, regional, and distant) were considered as an event. All analyses were carried out using Stata software, version 15 (StataCorp, 2017, Stata Statistical Software: Release 15, College Station, Texas, USA: StataCorp LP). The significance level was set at 5%.

Results

Clinicopathologic features of endometrial carcinoma and conventional prognostic stratification

Clinicopathologic characteristics of the 125 patients are shown in table 5. Median patient age at diagnosis was median 62.7 years. The median body mass index (BMI; kg/m2) was 27.5. Histologic classification includes 90 (72%) endometrioid, 17 (13.6%) dedifferentiated/undifferentiated, 15 (12.0%) serous, and 3 (2.4%) clear cell endometrial carcinomas. Grade distribution is homogeneous and includes 36 (28.8%) grade 1, 35 (28.0%) grade 2 and 54 (43.2%) grade 3. Lymph node metastases are present in 24 (19.2%) patients.

Applying FIGO stage/AJCC 8th ed., 71 (56.8%) patients were stage IA, 18 (14.4%) stage IB, 4 (3.2%) stage II, 30 (24.0%) stage III and 2 (1.6%) stage IV. Median follow-up was 19.1 months (range 1-119.5). Eleven (8.8%) patients developed disease progression during follow-up (1 local and 10 distant recurrences), and 6 (4.8%) patients died of the disease. FIGO stage was significantly associated with disease-free survival (log-rank: $\chi^2 = 14.64$, P-value <0.001) and overall survival (log-rank: $\chi^2 = 11.64$, P-value = 0.003) (see figures 3a and 3b).

Table 5. Clinicopathologic characteristics of the study sample. Values are counts (percentages) or mean ± standard deviation [interquartile range].

Clinicopathologic characteristics	*n* = 125 (%)
Age, years	62.7 ± 10.7 [56–71]
Body mass index, kg/m²	27.5 ± 6.6 [22.8–30.1]
Tumor type	
Endometrioid	90 (72.0)
Dedifferentiated/Undifferentiated	17 (13.6)
Serous	15 (12.0)
Clear cell	3 (2.4)
Grade	
1	36 (28.8)
2	35 (28.0)
3	54 (43.2)
Depth of invasion	
<50%	90 (72.0)
≥50%	35 (28.0)
Lymphovascular space invasion (LVSI)	
Absent	88 (70.4)
Present	37 (29.6)
Lymph node status	
Negative	95 (76.0)
Positive	24 (19.2)
Unknown/Not tested	6 (4.8)
FIGO stage	
IA	71 (56.8)
IB	18 (14.4)
II	4 (3.2)
III	30 (24.0)
IV	2 (1.6)
ESMO (2016)	
Low	18 (14.4)
Intermediate	8 (6.4)
High–intermediate	42 (33.6)
High	57 (45.6)
Extensive necrosis	
Absent	66 (52.8)
Present	59 (47.2)
MELF	
Absent	79 (63.2)
Present	46 (36.8)
Tumor budding	
Absent	73 (58.4)
Present	52 (41.6)
sTILs	
Low	36 (28.8)
High	89 (71.2)
iTILs	
Low	39 (31.2)
High	86 (68.8)
Recurrence	
Absent	114 (91.2)
Present	11 (8.8)

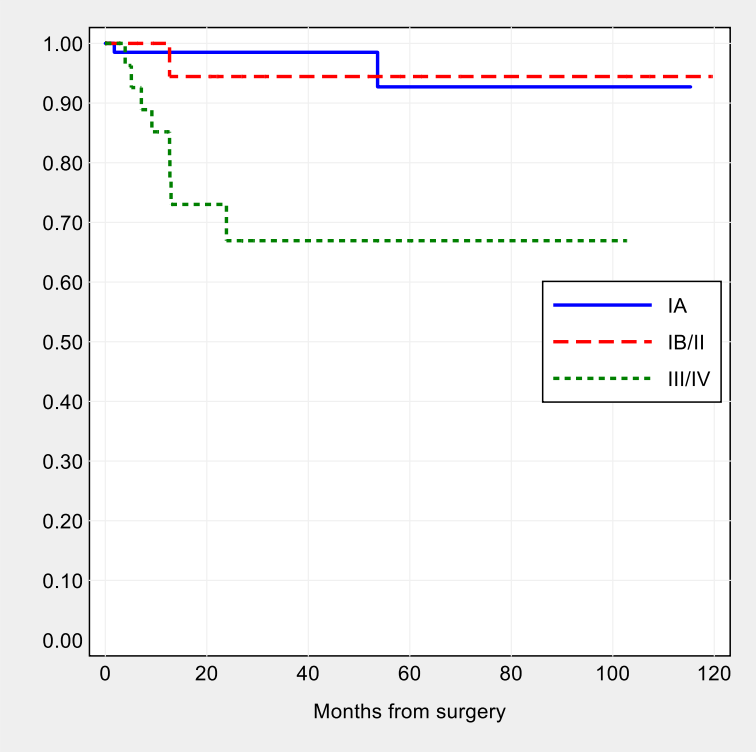

Figure 3a. Kaplan–Meier estimates of disease-free survival by FIGO stage.

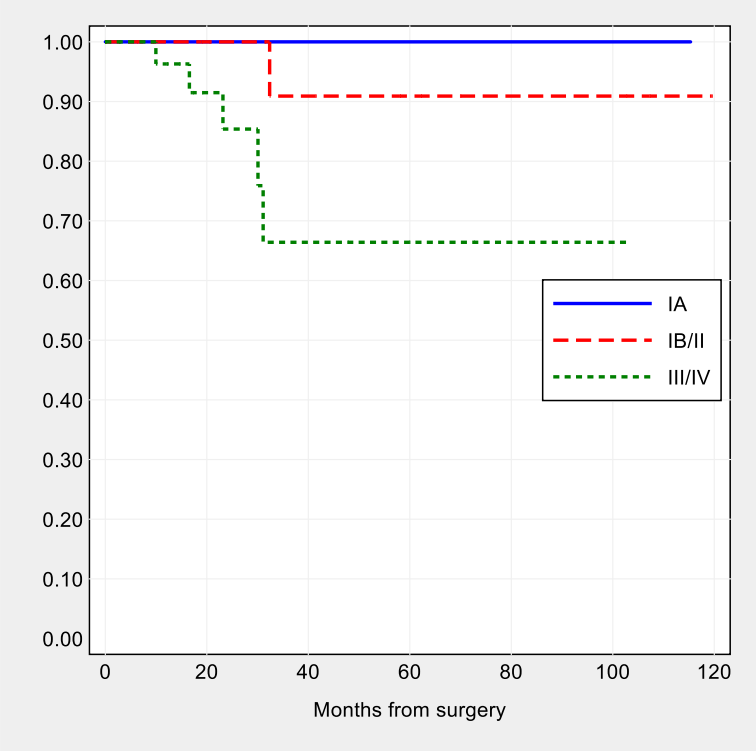

Figure 3b. Kaplan–Meier estimates of overall survival by FIGO stage.

Applying ESMO 2016 risk stratification criteria, 18 (14.4%) carcinomas were low risk, 8 (6.4%) intermediate risk, 42 (33.6%) high-intermediate and 57 (45.6%) high risk. ESMO 2016 risk groups were significantly correlated with disease-free survival (log-rank: $\chi^2 = 9.47$, P-value = 0.024), but not with overall survival (log-rank: $\chi^2 = 5.63$, P-value = 0.131) (see figures 4a and 4b).

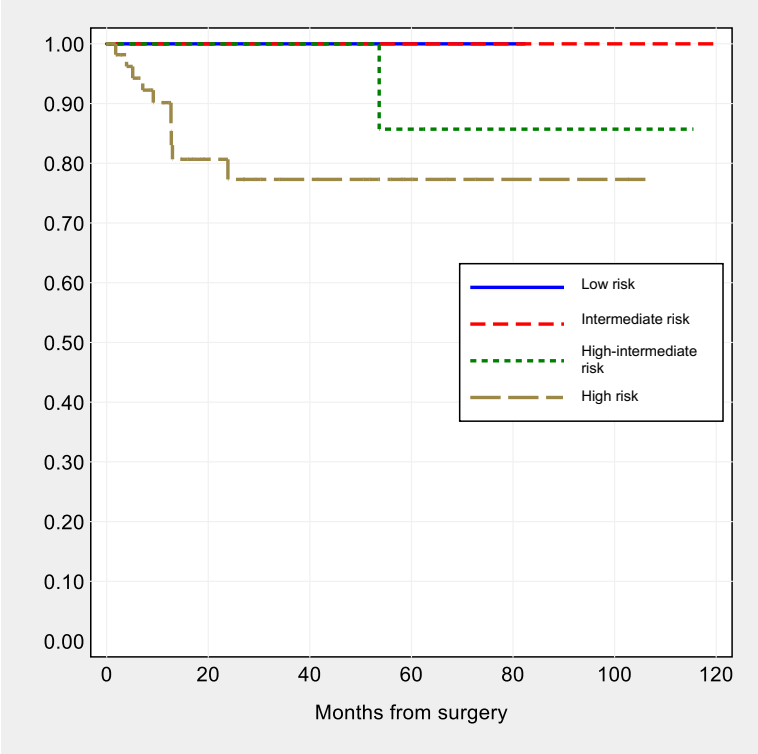

Figure 4a. Kaplan–Meier estimates of disease-free survival by ESMO risk groups.

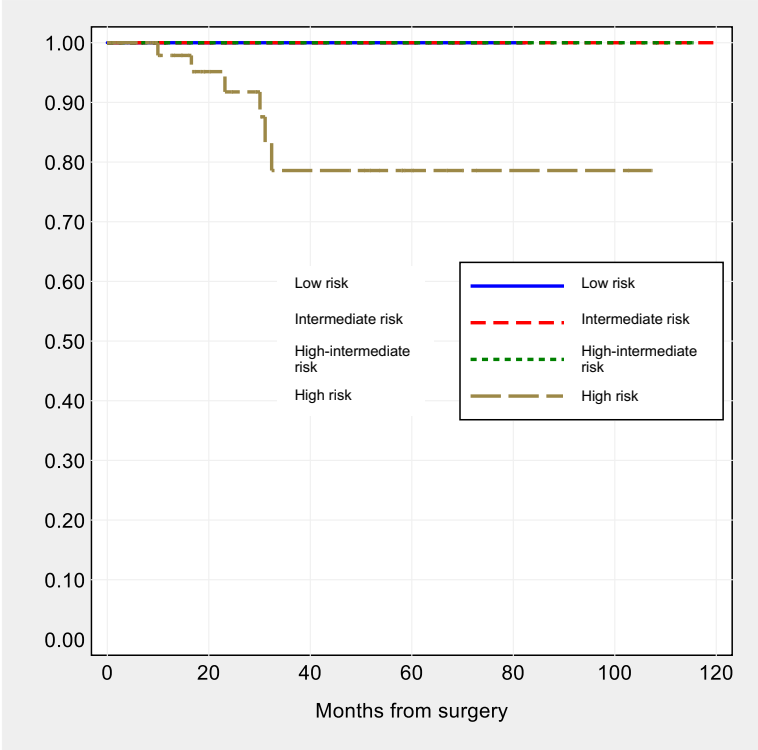

Figure 4b. Kaplan–Meier estimates of overall survival by ESMO risk groups.

Molecular TCGA group assignment

Surrogate TCGA molecular typing of the 125 EC cases classified tumors into the following groups: 9 (7.2%) *POLE* group, 41 (32.8%) MMRd group, 26 (20.8%) p53abn group, 49 (39.2%) NSMP group. The association between TCGA molecular groups and clinicopathologic parameters (BMI, histotype, grade, FIGO stage, MELF, tumor budding, TILs, mitoses, Ki67 proliferative index) are shown in table 6. Nine cases (7.2%) show more than one molecular feature (so called "multiple classifier" tumors): 2 tumors are *POLE*-p53abn, 1 tumor is *POLE*-MMRd, 1 tumor is *POLE*-MMRd-p53abn, 5 tumors are MMRd-p53abn.

Table 6. Clinicopathologic characteristics of surrogate TGCA molecular groups. Values are counts (percentages) or mean ± standard deviation [interquartile range].

Clinicopathologic characteristics	***POLE*** (n = 9; 7.2%)	**MMRd** (n = 41; 32.8%)	**p53abn** (n = 26; 20.8%)	**NSMP** (n = 49; 39.2%)	***P*-value**
Age, years	61.2 ± 13.9 [52–71]	64.2 ± 10.0 [57–73]	65.0 ± 10.0 [59–74]	60.6 ± 11.0 [55–69]	0.266
Body mass index, kg/m²	25.3 ± 4.6 [21.3–28.1]	26.8 ± 6.1 [22.7–28.2]	25.4 ± 4.1 [22.8–27.2]	29.5 ± 7.8 [24.0–33.8]	0.104
Tumor type					<0.001
Endometrioid	8 (88.9)	30 (73.2)	7 (26.9)	45 (91.8)	
Dedifferentiated/ Undifferentiated	1 (11.1)	11 (26.8)	1 (3.8)	4 (8.2)	
Serous	0 (0.0)	0 (0.0)	15 (57.7)	0 (0.0)	
Clear cell	0 (0.0)	0 (0.0)	3 (11.5)	0 (0.0)	
Heterogeneity	4 (44.4)	21 (51.2)	10 (38.5)	14 (28.6)	0.168
Grade					<0.001
1	2 (22.2)	11 (26.8)	1 (3.8)	22 (44.9)	
2	3 (33.3)	14 (34.1)	0 (0.0)	18 (36.7)	
3	4 (44.4)	16 (39.0)	25 (96.2)	9 (18.4)	
Depth of invasion ≥50%	1 (11.1)	15 (36.6)	9 (34.6)	10 (20.4)	0.208
LVSI	2 (22.2)	14 (34.1)	11 (42.3)	10 (20.4)	0.196
Lymph node status					0.141
Negative	8 (88.9)	31 (75.6)	15 (57.7)	41 (83.7)	
Positive	1 (11.1)	8 (19.5)	10 (38.5)	5 (10.2)	
FIGO stage					0.011
IA	5 (55.6)	19 (46.3)	12 (46.2)	35 (71.4)	
IB/II	2 (22.2)	12 (29.3)	1 (3.8)	7 (14.3)	
III	2 (22.2)	9 (22.0)	12 (46.2)	7 (14.3)	
IV	0 (0.0)	1 (2.4)	1 (3.8)	0 (0.0)	
Extensive necrosis	6 (66.7)	23 (56.1)	11 (42.3)	19 (38.8)	0.235
MELF	5 (55.6)	24 (58.5)	3 (11.5)	14 (28.6)	<0.001
Tumor budding	7 (77.8)	23 (56.1)	8 (30.8)	14 (28.6)	0.004
High sTILs	9 (100.0)	35 (85.4)	19 (73.1)	26 (53.1)	0.001
High iTILs	9 (100.0)	37 (90.2)	17 (65.4)	23 (46.9)	<0.001
Mitoses/10 HPF	78.1 ± 34.5 [50–103]	55.3 ± 23.7 [40–70]	86.3 ± 43.7 [45–130]	33.3 ± 27.7 [10–42]	<0.001
Ki67 proliferation index	58.5 ± 14.9 [55.1–68.2]	57.9 ± 14.9 [47.1–69.6]	56.0 ± 16.7 [49.3–69.7]	36.6 ± 18.3 [23.3–50.0]	<0.001

The features of the EC cases according to the surrogate TCGA molecular classification are as follows:

1. *POLE*-mutated tumors. Predominantly endometrioid, grade 3 and morphologically heterogeneous in half of the cases, statistically associated with characteristic myometrial infiltration patterns (MELF and tumor budding), intense intra- and peri-tumoral lymphocytic infiltrate (iTILs and sTILs), high mitotic rate and high Ki67 proliferative index (see figure 5). In the *POLE* group, lymph node metastases are present in one of 9 cases (11.1%).

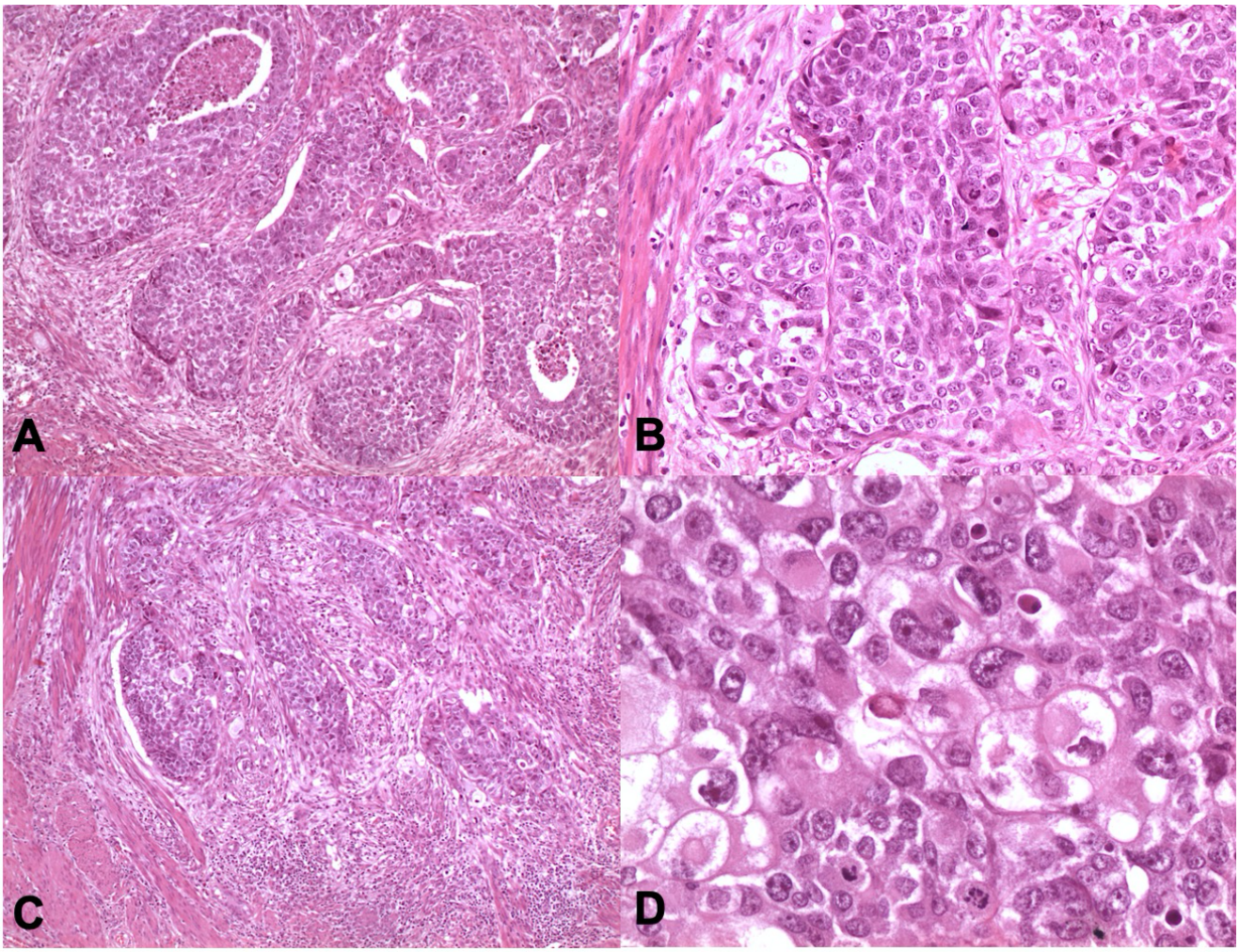

Figure 5. *POLE*-mutated endometrioid carcinomas. *POLE* carcinomas may have eosinophilic tumor cells with marked atypical nuclei and lymphoid infiltrate (A and C x100 magnification, B x200 magnification, D x400 magnification; Hematoxylin and eosin - H&E).

2. MMRd tumors. Characterized by endometrioid or dedifferentiated/undifferentiated histotypes, homogeneous histologic grade distribution, association with MELF pattern of myometrial invasion, tumor budding and high iTILs /sTILs (see figure 6). Lymph node metastases present in 8 cases (19.5%).

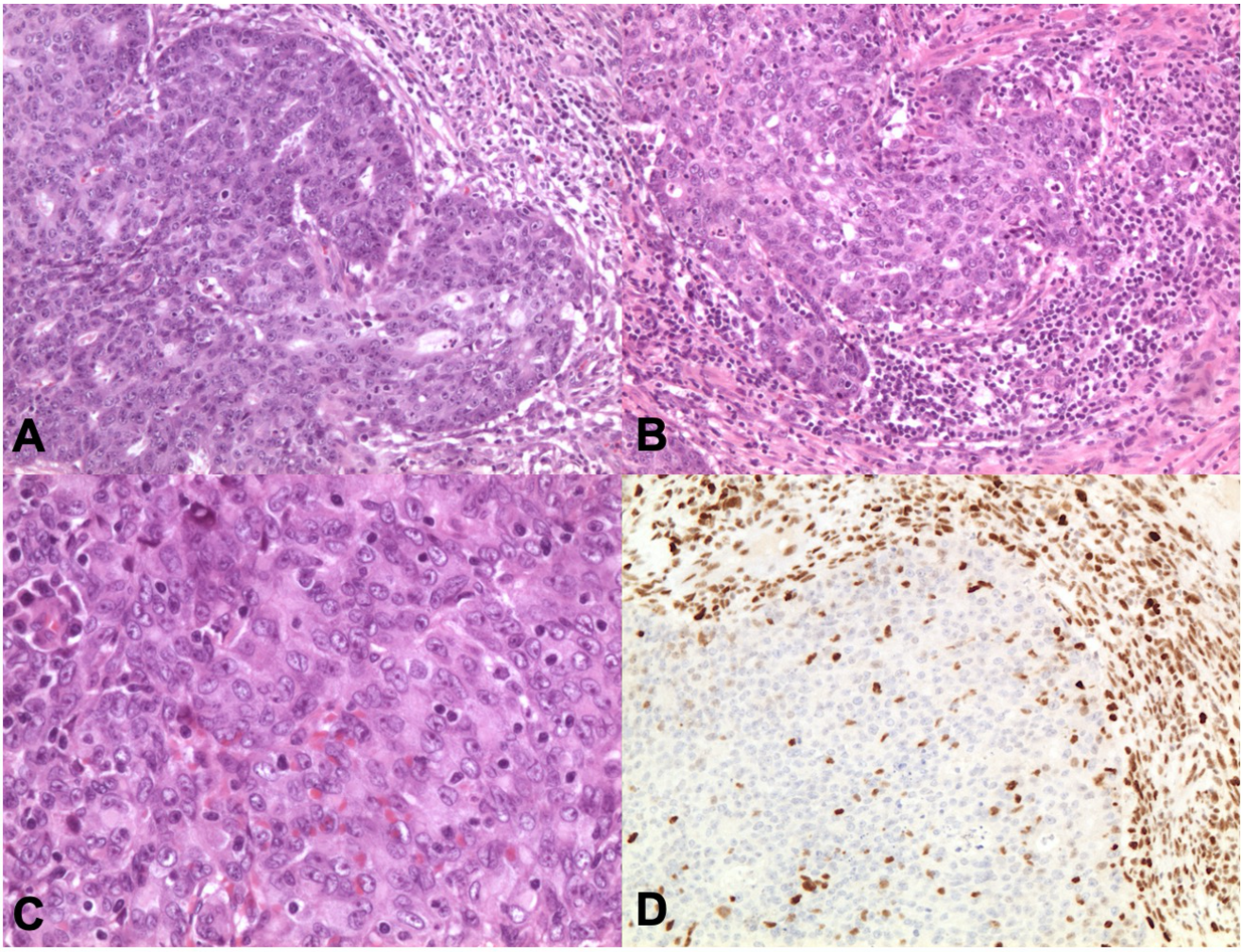

Figure 6. MMRd endometrioid carcinoma. The tumor shows numerous intra- and peritumoural tumour infiltrating lymphocytes (A and B x200 magnification, C x400 magnification; Hematoxylin and eosin - H&E) and diffuse immunohistochemical nuclear loss of MLH1 (D x400 magnification).

3. p53abn tumors. Significantly associated with serous histotype, grade 3, high mitotic rate and high Ki67 proliferative index (see figure 7). Metastatic lymph nodes in 10 cases (38.5%).

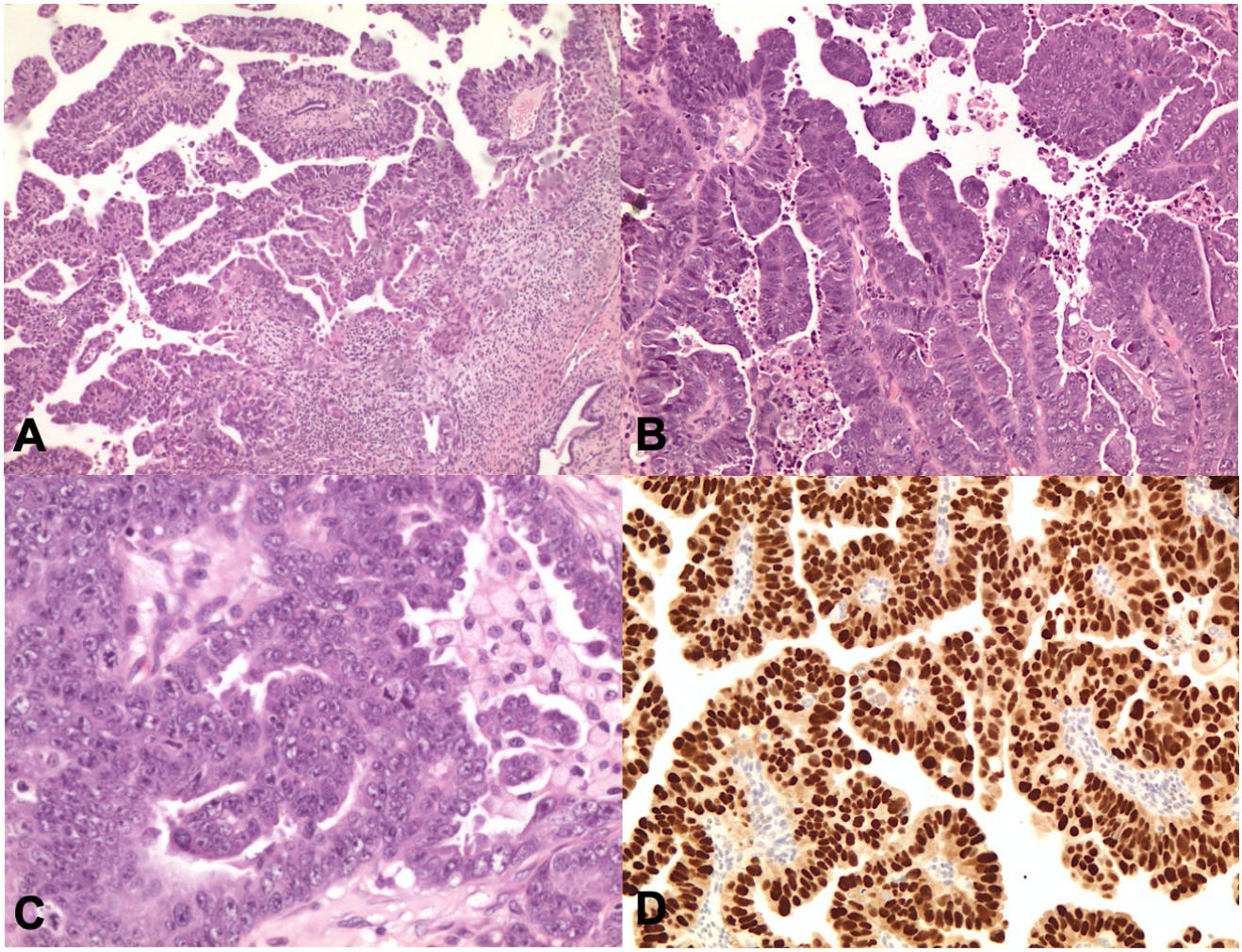

Figure 7. p53 abn carcinoma. Tumor have a serous histotype with marked nuclear pleomorphism, macronucleoli, and conspicuous mitotic activity (A x100 magnification, B x200 magnification, C x400 magnification; Hematoxylin and eosin - H&E) and p53 abnormal/mutant-like (D x200 magnification).

4. NSMP tumors. Endometrioid, more frequently grade 1-2, lower mitotic activity and Ki67 proliferative index (compared with the other EC groups), with metastatic lymph node metastatic in 5 cases (10.5%) (see Figure 8).

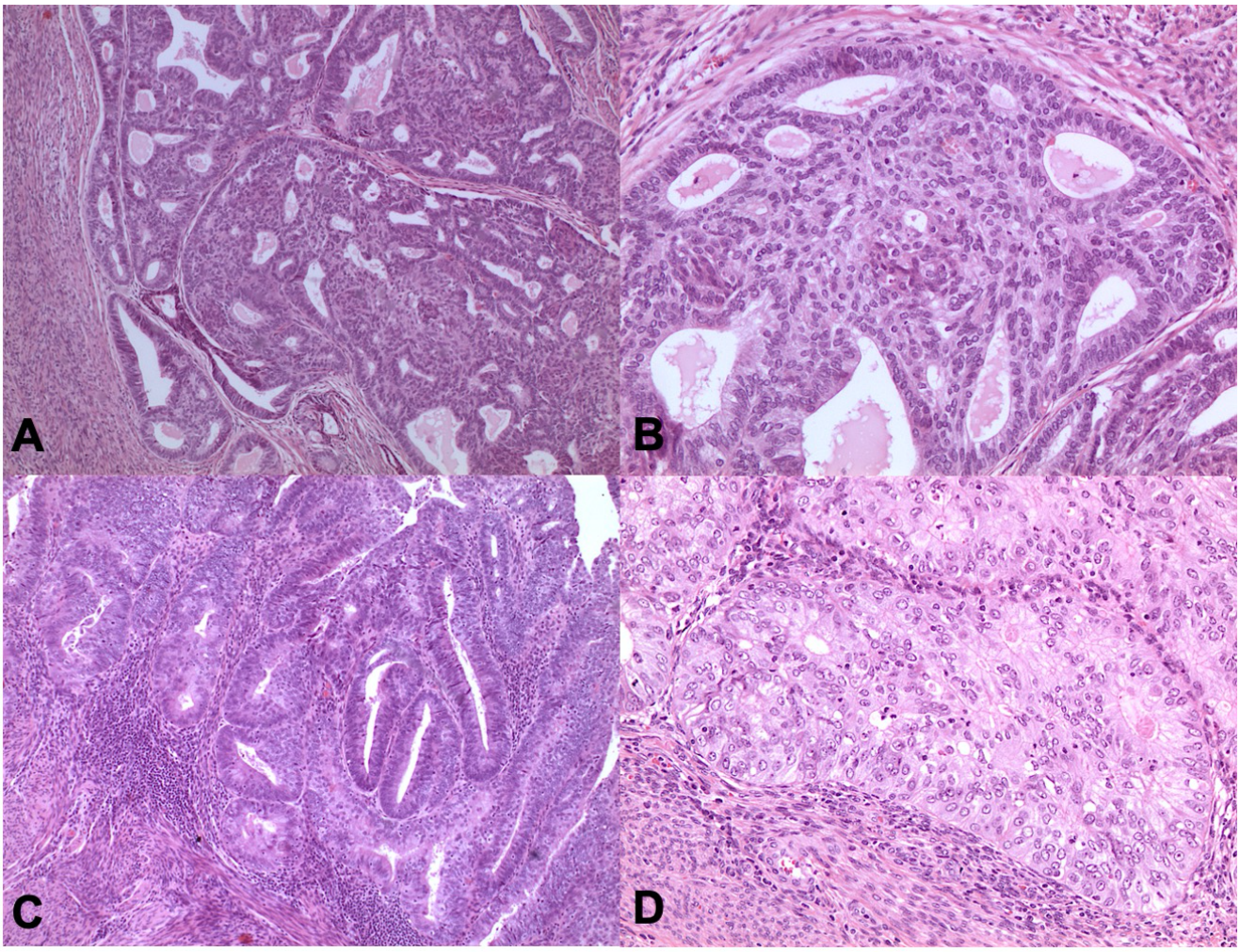

Figure 8. NSMP tumors are prevalently endometrioid, low grade morphology (A and C x100 magnification, B and D x200 magnification; Hematoxylin and eosin - H&E).

Prognostic impact of the surrogate TCGA molecular group classification: *POLE* tumors show the most favorable outcome, without any recurrence, while recurrent disease is observed in 3/41 (7.3%) MMRd, 3/26 (11.5%) p53abn, 5/49 (10.2%) NSMP subtypes. The patient outcome by molecular classification (figure 9) is consistent with that previously reported [48-50], but in this series does not reach statistical significance for disease-free survival (log-rank: $\chi^2 = 1.29$, P-value = 0.730) and for overall survival (log-rank: $\chi^2 = 1.98$, P-value = 0.576).

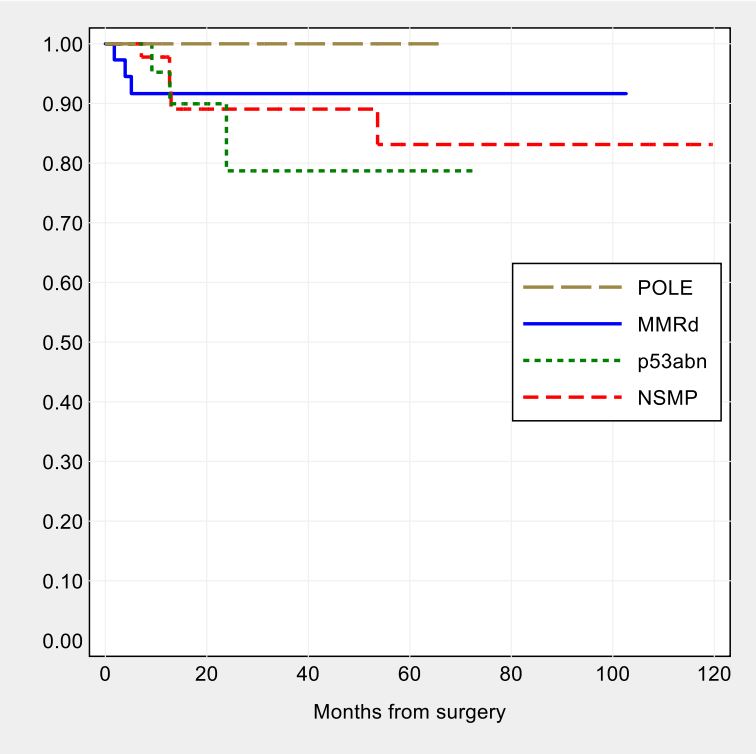

Figure 9a. Kaplan–Meier estimates of disease-free survival by surrogate TCGA molecular groups.

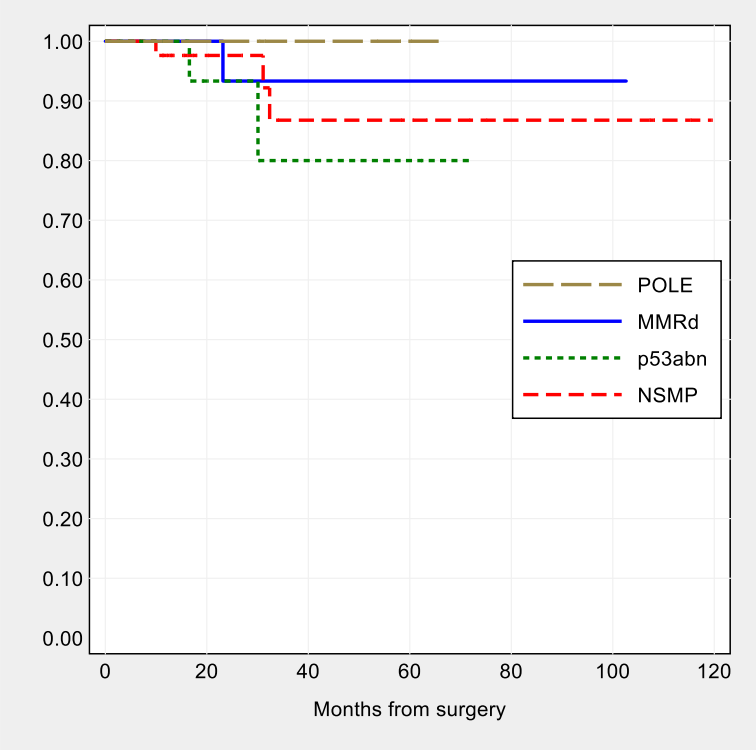

Figure 9b. Kaplan–Meier estimates of overall survival by surrogate TCGA molecular groups.

Considering ESMO high-intermediate and high risk groups, surrogate TCGA molecular classification was not statistically correlated with disease-free survival and overall survival (log-rank: $\chi^2 = 1.45$, P-value = 0.694 and $\chi^2 = 2.19$, P-value = 0.534 ,respectively) (see figure 10).

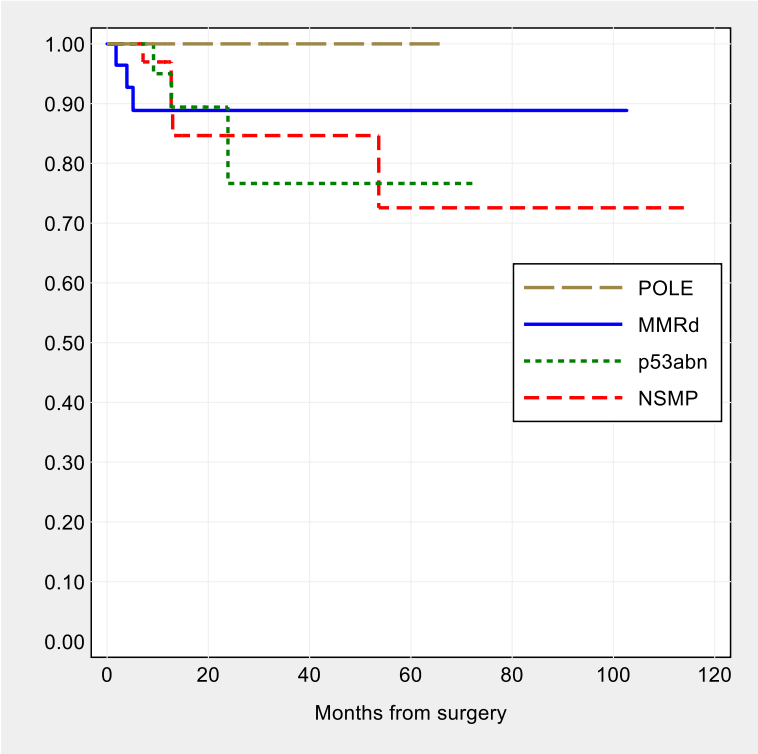

Figure 10a. Kaplan–Meier estimates of disease-free survival in patients at high-intermediate and high risk according to ESMO (n = 99), by surrogateTCGA molecular groups.

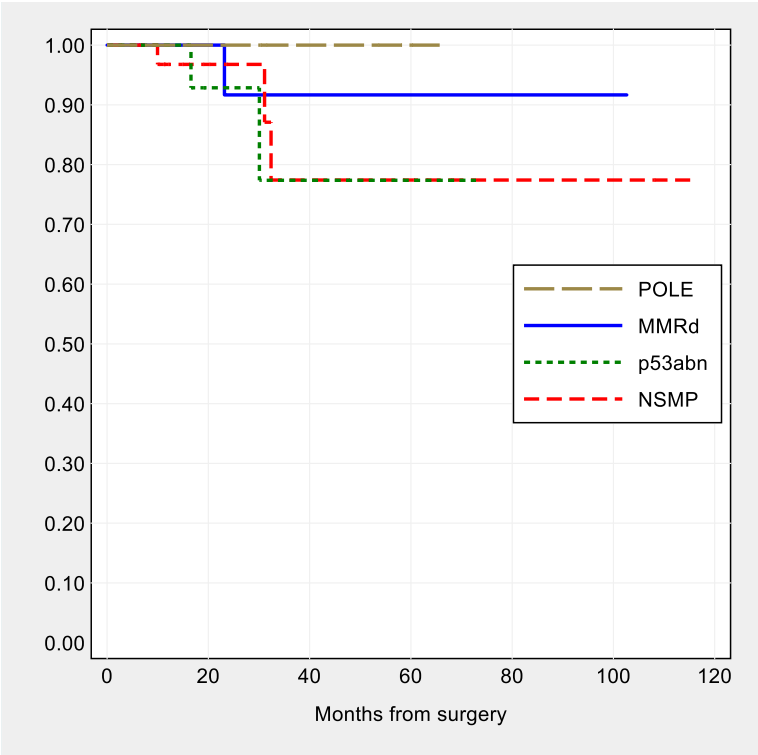

Figure 10b. Kaplan–Meier estimates of overall survival in patients at high-intermediate and high risk according to ESMO (n = 99), by TCGA molecular groups.

CTNNB1 mutations/ β-catenin abnormal expression

Of the 125 endometrial carcinomas examined, 21 (16.8%) tumors carry exon 3 *CTNNB1* mutations and concomitant nuclear expression of β-catenin. For the *CTNNB1* mutant ECs, nuclear localization of β-catenin in neoplastic cells ranges from 5% to 60% (mean 19.8%). Clinicopathologic features of endometrial carcinoma associated with *CTNNB1* mutations/nuclear expression of β-catenin are shown in table 7. In summary, β-catenin mutated cases are characterized by young age at diagnosis, high BMI, low mitotic rate and Ki67 proliferative index, no tumor necrosis, low TILs counts, and prevalently encompass into the NSMP molecular group (16/21 cases).

Table 7. Clinicopathologic characteristics of *CTNNB1* mutated/β-catenin abnormal versus *CTNNB1* wild-type/β-catenin normal carcinomas. Values are counts (percentages) or mean ± standard deviation [interquartile range].

Characteristics	***CTNNB1* mutation/ β-catenin abnormal** (*n* = 21; 16.8%)	***CTNNB1* wild-type/ β-catenin normal** (*n* = 104; 83.2%)	***P*-value**
Age, years	54.9 ± 12.9 [44–64]	64.3 ± 9.6 [58–71.5]	<0.001
Body mass index, kg/m²	30.6 ± 7.8 [24.6–34.2]	26.8 ± 6.1 [22.7–29.3]	0.016
Tumor type			0.224
Endometrioid	17 (81.0)	73 (70.2)	
Dedifferentiated/ Undifferentiated	4 (19.0)	13 (12.5)	
Serous	0 (0.0)	15 (14.4)	
Clear cell	0 (0.0)	3 (2.9)	
TGCA molecular group			0.001
POLE	1 (4.8)	8 (7.7)	
MMRd	4 (19.0)	37 (35.6)	
p53abn	0 (0.0)	26 (25.0)	
NSMP	16 (76.2)	33 (31.7)	
Heterogeneity	7 (33.3)	42 (40.4)	0.546
Grade			0.071
1	10 (47.6)	26 (25.0)	
2	6 (28.6)	29 (27.9)	
3	5 (23.8)	49 (47.1)	
Depth of invasion ≥50%	5 (23.8)	30 (28.8)	0.639
Lymphovascular space invasion	5 (23.8)	32 (30.8)	0.524
Lymph node status			0.260
Negative	19 (90.5)	76 (73.1)	
Positive	2 (9.5)	22 (21.2)	
Unknown/Not tested	0 (0.0)	6 (5.8)	
FIGO stage			0.663
IA	14 (66.7)	57 (54.8)	
IB/II	4 (19.0)	18 (17.3)	
III	3 (14.3)	27 (26.0)	
IV	0 (0.0)	2 (1.9)	
Extensive necrosis	7 (33.3)	52 (50.0)	0.163
MELF	7 (33.3)	39 (37.5)	0.718
Tumor budding	6 (28.6)	46 (44.2)	0.184
High sTILs	11 (52.4)	78 (75.0)	0.037
High iTILs	9 (42.9)	77 (74.0)	0.005
Mitoses/10 HPF	37.6 ± 32.0 [10–60]	58.2 ± 37.1 [30–81]	0.019
Ki67 proliferation index	41.8 ± 22.5 [19.7–63.1]	50.9 ± 18.3 [38.0–67.6]	0.049

Considering the prognostic role of *CTNNB1* mutations reported in the literature [19, 44, 51], and its association with the NSMP group, this latter was divided into two subgroups: 15/43 (34.9%) β-catenin abnormal (β-CATabn) cases, and 28/43 (65.1%) NSMP *CTNNB1* wild type (NSMP) cases. By integrating

the surrogate TCGA molecular groups with the β-CATabn subgroup, β-catenin mutated tumors are similar to those of the NSMP subtype, except for lower mitotic rate and Ki67 proliferative index (see table 8).

Table 8. Surrogate TCGA molecular groups including β-catenin altered subgroup. Values are counts (percentages) or mean ± standard deviation [interquartile range].

Clinicopathologic characteristics	***POLE*** (*n* = 9; 7.2%)	**MMRd** (*n* = 41; 32.8%)	**p53abn** (*n* = 26; 20.8%)	**β-CATabn** (*n* = 16; 12.8%)	**NSMP** (*n* = 33; 26.4%)	***P*-value**
Age, years	61.2±13.9 [52–71]	64.2±10.0 [57–73]	65.0±10.0 [59–74]	54.3±12.9 [44–63]	63.6±8.5 [58–70]	0.067
Body mass index, kg/m²	25.3±4.6 [21.3–28.1]	26.8±6.1 [22.7–28.2]	25.4±4.1 [22.8–27.2]	29.0±6.7 [22.5–33.5]	29.7±8.3 [24.2–36.1]	0.187
Tumor type						<0.001
Endometrioid	8 (88.9)	30 (73.2)	7 (26.9)	14 (87.5)	31 (93.9)	
Dedifferentiated/ Undifferentiated	1 (11.1)	11 (26.8)	1 (3.8)	2 (12.5)	2 (6.1)	
Serous	0 (0.0)	0 (0.0)	15 (57.7)	0 (0)	0 (0)	
Clear cell	0 (0.0)	0 (0.0)	3 (11.5)	0 (0)	0 (0)	
Heterogeneity	4 (44.4)	21 (51.2)	10 (38.5)	5 (31.3)	9 (27.3)	0.290
Grade						<0.001
1	2 (22.2)	11 (26.8)	1 (3.8)	8 (50.0)	14 (42.4)	
2	3 (33.3)	14 (34.1)	0 (0.0)	5 (31.3)	13 (39.4)	
3	4 (44.4)	16 (39.0)	25 (96.2)	3 (18.8)	6 (18.2)	
Depth of invasion ≥50%	1 (11.1)	15 (36.6)	9 (34.6)	3 (18.8)	7 (21.2)	0.361
Lymphovascular space invasion	2 (22.2)	14 (34.1)	11 (42.3)	3 (18.8)	7 (21.2)	0.350
Lymph node status						0.193
Negative	8 (88.9)	31 (75.6)	15 (57.7)	15 (93.8)	26 (78.8)	
Positive	1 (11.1)	8 (19.5)	10 (38.5)	1 (6.3)	4 (12.1)	
Unknown/Not tested	0 (0.0)	2 (4.9)	1 (3.8)	0 (0.0)	3 (9.1)	
FIGO stage						0.048
IA	5 (55.6)	19 (46.3)	12 (46.2)	11 (68.8)	24 (72.7)	
IB/II	2 (22.2)	12 (29.3)	1 (3.8)	3 (18.8)	4 (12.1)	
III	2 (22.2)	9 (22.0)	12 (46.2)	2 (12.5)	5 (15.2)	
IV	0 (0.0)	1 (2.4)	1 (3.8)	0 (0.0)	0 (0.0)	
Extensive necrosis	6 (66.7)	23 (56.1)	11 (42.3)	4 (25.0)	15 (45.5)	0.195
MELF	5 (55.6)	24 (58.5)	3 (11.5)	4 (25.0)	10 (30.3)	0.001
Tumor budding	7 (77.8)	23 (56.1)	8 (30.8)	4 (25.0)	10 (30.3)	0.011
High sTILs	9 (100.0)	35 (85.4)	19 (73.1)	7 (43.8)	19 (57.6)	0.002
High iTILs	9 (100.0)	37 (90.2)	17 (65.4)	4 (25.0)	19 (57.6)	<0.001
Mitoses/10 HPF	78.1±34.5 [50–103]	55.3±23.7 [40–70]	86.3±43.7 [45–130]	30.5±30.1 [9–44]	34.6±26.8 [20–40]	<0.001
Ki67 proliferation index	58.5±14.9 [55.1–68.2]	57.9±14.9 [47.1–69.6]	56.0±16.7 [49.3–69.7]	35.9±21.6 [17.1–58.4]	36.9±16.6 [25.3–42.7]	<0.001

ARID1A mutations/ ARID1A loss of expression

IHC ARID1A loss is present in 69/125 (55.2%) and it is concordant with *ARID1A* mutations. The clinicopathologic features associated with *ARID1A* mutation are shown in table 9. ARID1A alteration is significantly associated with endometrioid and dedifferentiated/undifferentiated histotypes, MMRd and *POLE* molecular subgroups, MELF pattern of invasion, high TILs and high ki67 proliferative index.

Table 9. Clinicopathologic characteristics of *ARID1A* altered versus *ARID1A* wild-type carcinomas. Values are counts (percentages) or mean ± standard deviation [interquartile range].

Clinicopathologic characteristics	***ARID1A* altered** (*n* = 69; 55.2%)	***ARID1A* wild-type** (*n* = 56; 44.8%)	***P*-value**
Age, years	63.0 ± 9.6 [56–71]	62.4 ± 12.0 [55–72]	0.742
Body mass index, kg/m²	27.9 ± 6.8 [22.8–31.1]	26.9 ± 6.3 [22.6–29.1]	0.362
Tumor type			0.002
Endometrioid	54 (78.3)	36 (64.3)	
Dedifferentiated/ Undifferentiated	12 (17.4)	5 (8.9)	
Serous	3 (4.3)	12 (21.4)	
Clear cell	0 (0.0)	3 (5.4)	
TGCA molecular group			<0.001
POLE	8 (11.6)	1 (1.8)	
MMRd	33 (47.8)	8 (14.3)	
p53abn	3 (4.3)	23 (41.1)	
NSMP	25 (36.2)	24 (42.9)	
Heterogeneity	32 (46.4)	17 (30.4)	0.068
Grade			0.028
1	17 (24.6)	19 (33.9)	
2	26 (37.7)	9 (16.1)	
3	26 (37.7)	28 (50.0)	
Depth of invasion ≥50%	22 (31.9)	13 (23.2)	0.283
LVSI	25 (36.2)	12 (21.4)	0.071
Lymph node status			0.344
Negative	50 (72.5)	45 (80.4)	
Positive	14 (20.3)	10 (17.9)	
FIGO stage			0.850
IA	38 (55.1)	33 (58.9)	
IB/II	14 (20.3)	8 (14.3)	
III	16 (23.2)	14 (25.0)	
IV	1 (1.4)	1 (1.8)	
Extensive necrosis	35 (50.7)	24 (42.9)	0.381
MELF	36 (52.2)	10 (17.9)	<0.001
Tumor budding	35 (50.7)	17 (30.4)	0.022
High sTILs	56 (81.2)	33 (58.9)	0.006
High iTILs	57 (82.6)	29 (51.8)	<0.001
Mitoses/10 HPF	56.0 ± 29.6 [32–70]	53.2 ± 44.7 [15–90]	0.674
Ki67 proliferation index	54.2 ± 16.8 [39.7–67.6]	43.4 ± 20.7 [25.5–57.2]	0.002

Integrating *ARID1A* analysis in molecular subtyping, *ARID1A* alteration is found in 8/9 (88.9%) *POLE*, 33/41 (80.5%) MMRd, 3/26 (11.5%) p53abn, 19/33 (57.6%) NSMP and in 7/16 (43.8%) β -CATabn group tumors. Of note, ARID1A clonal loss ("clonal loss" IHC pattern) corresponding to subclonal inactivating *ARID1A* mutations is identified in 27/69 (39.1%) mutated tumors: 5 *POLE*, 11 MMRd, 2 p53abn, 5 NSMP, 4 β -CATabn. In the *POLE*, MMRd and p53abn groups, ARID1A loss/mutation is not associated with specific clinicopathologic features.

In contrast, in the β -CATabn subgroup, loss/mutation of *ARID1A* is associated with older age (p=0.044), high grade (p=0.001), extensive necrosis (p=0.019), tumor budding (p=0.019), high scores for sTILs and iTILs (p=0.009 and p=0.012, respectively), high mitotic rate and high Ki-67 proliferative index (p=0.001 and p=0.003, respectively). *ARID1A* alteration in NSMP (NSMP_A) group correlates with high Ki-67 proliferative index and with tumor recurrence (see table 10).

Table 10. NSMP subgroups by β-catenin and *ARID1A* alterations. Values are counts (percentages) or mean ± standard deviation [interquartile range].

Clinicopathologic characteristics	β-catenin abnormal subgroup (*n* = 16)			NSMP subgroup (*n* = 33)		
	β-CATabn (*n* = 9)	β-CATabn_A (*n* = 7)	*P*-value	NSMP (*n* = 14)	NSMP_A (*n* = 19)	*P*-value
Age, years	49 ± 13 [40–54]	61 ± 10 [55–73]	0.044	66 ± 10 [55–75]	62 ± 7 [58–69]	0.352
Body mass index, kg/m²	27.3 ± 7.8 [20.3–29.1]	31.1 ± 4.7 [28.1–33.8]	0.186	27.6 ± 6.1 [23.4–28.9]	31.3 ± 9.5 [24.2–37.3]	0.229
Tumor type			0.175			1.000
Endometrioid	9 (100)	5 (71)		13 (93)	18 (95)	
Dedifferentiated/Un-differentiated	0 (0)	2 (29)		1 (7)	1 (5)	
Heterogeneity	1 (11)	4 (57)	0.106	2 (14)	7 (37)	0.241
Grade			0.001			0.391
1	8 (89)	0 (0)		8 (57)	6 (32)	
2	1 (11)	4 (57)		4 (29)	9 (47)	
3	0 (0)	3 (43)		2 (14)	4 (21)	
Depth of invasion ≥50%	0 (0)	3 (43)	0.062	3 (21)	4 (21)	1.000
Lymphovascular space invasion	0 (0)	3 (43)	0.062	2 (14)	5 (26)	0.670
Lymph node status			0.437			0.830
Negative	9 (100)	6 (86)		12 (86)	14 (74)	
Positive	0 (0)	1 (14)		1 (7)	3 (16)	
Unknown/Not tested	0 (0)	0 (0)		1 (7)	2 (11)	
FIGO stage			0.758			1.000
IA	7 (78)	4 (57)		10 (71)	14 (74)	
IB/II	1 (11)	2 (29)		2 (14)	2 (11)	
III	1 (11)	1 (14)		2 (14)	3 (16)	
Extensive necrosis	0 (0)	4 (57)	0.019	6 (43)	9 (47)	1.000
MELF	2 (22)	2 (29)	1.000	3 (21)	7 (37)	0.455
Tumor budding	0 (0)	4 (57)	0.019	3 (21)	7 (37)	0.455
High sTILs	1 (11)	6 (86)	0.009	7 (50)	12 (63)	0.497
High iTILs	0 (0)	4 (57)	0.019	6 (43)	13 (68)	0.173
Mitoses/10 HPF	9.3 ± 4.8 [5–10]	57.7 ± 26.3 [42–80]	0.001	31.1 ± 33.7 [10–40]	37.2 ± 21.0 [24–50]	0.100
Ki67 proliferation index	20.7 ± 11.2 [13.8–29.6]	55.4 ± 14.5 [49.5–64.8]	0.003	31.4 ± 18.8 [19.3–36.9]	41.5 ± 13.5 [33.7–42.7]	0.037

The heatmap summarizes mutation status/IHC alterations in the different molecular groups (figure 11). All cases with *TP53* mutation showed an immunohistochemical overexpression of p53. Nine cases showed overexpression of p53 protein in absence of an identifiable mutation: this discrepancy may be due to the presence of macrodeletions or to gene regions not covered by the NGS panel. All cases with pathogenic variant of *ARID1A* showed loss of immunohistochemical expression. *ARID1A* mutation was

not idenfified by sequencing in eight cases with subclonal loss of ARID1A: this could be explained by the limitation of NGS sensitivity. All tumors carry exon 3 *CTNNB1* mutations exhibited concomitant nuclear expression of β-catenin in neoplastic cells (ranges from 5% to 60%). List of all variants identified (*POLE*, *TP53*, *KRAS*, *PIK3CA*, *CTNNB1*, *ARID1A*) are shown in Supplementary Table 2.

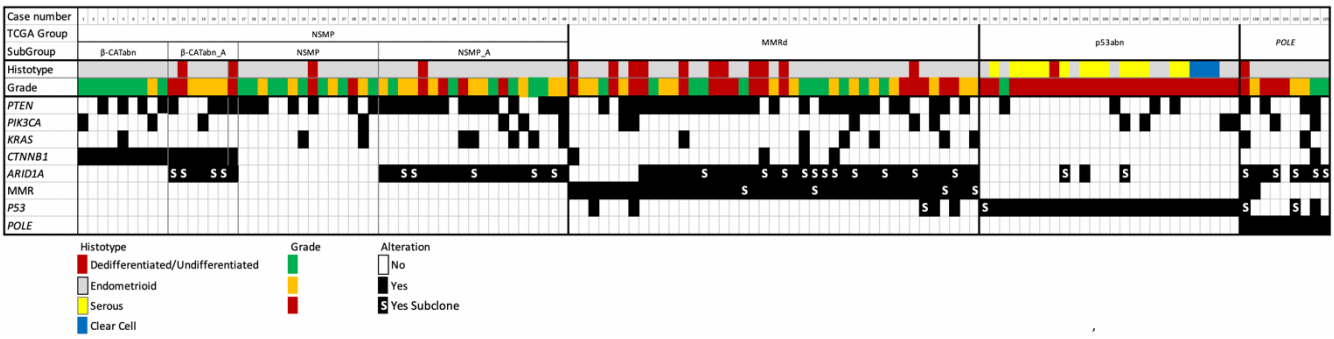

Figure 11. Immuno-molecular characterization of 125 endometrial carcinomas stratified according to histopathologic, immunophenotypic and molecular analyses.

Correlation of immuno-molecular subgroups with clinical outcome

The prognostic impact of surrogate TCGA molecular classification integrated with *CTNNB1*/β-catenin and *ARID1A* analyses was evaluated and the molecular subgroups tended to be associated with different disease-free survival (log-rank: $\chi^2 = 12.13$, P-value = 0.059), but not with overall survival (log-rank: $\chi^2 = 9.30$, P-value = 0.157) (see figures 12a and 12b).

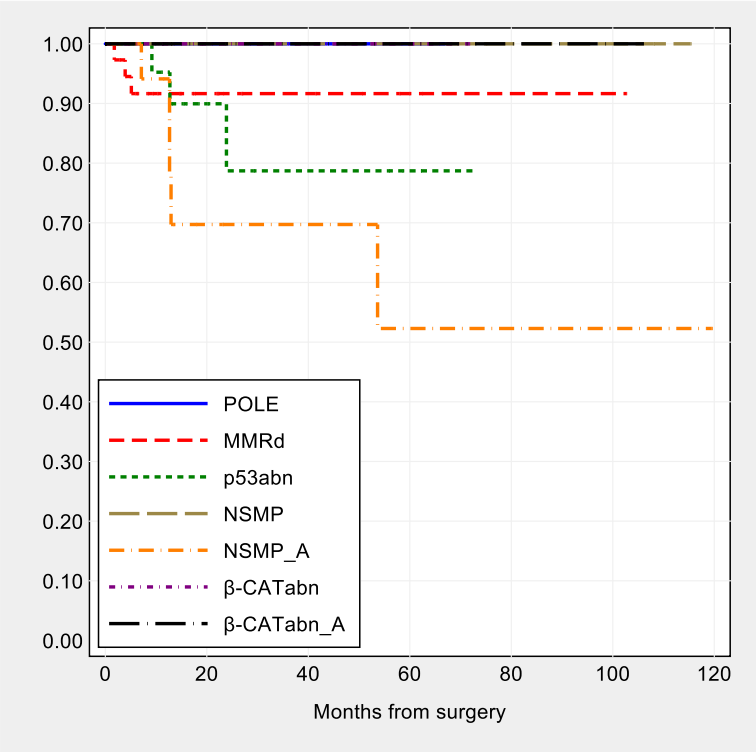

Figure 12a. Kaplan–Meier estimates of disease-free survival by molecular subgroup, including β-catenin and ARID1A alterations.

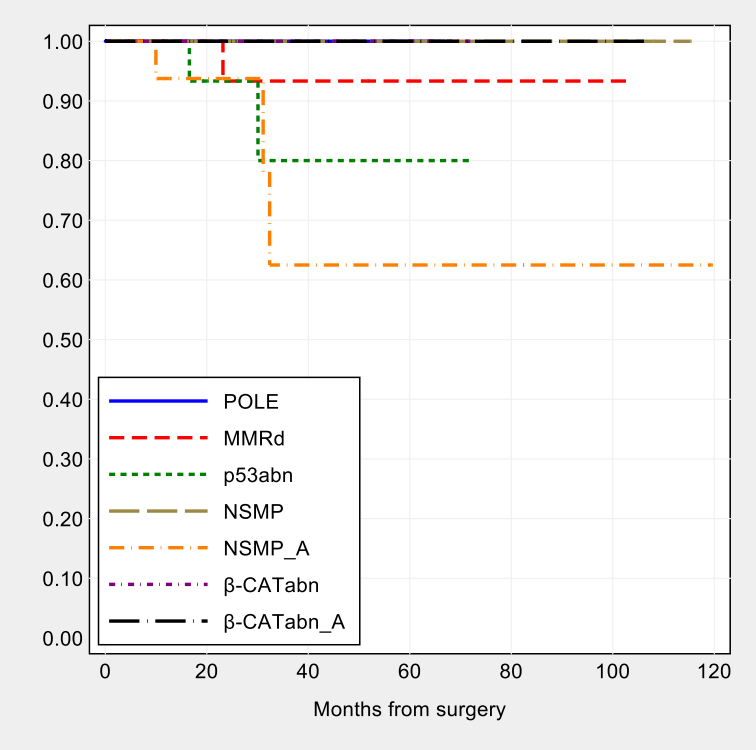

Figure 12b. Kaplan–Meier estimates of overall survival by molecular subgroup, including β-catenin and *ARID1A* alterations.

Considering the disease-free survival, if we limit the analysis to ESMO high-intermediate and high risk groups, *POLE*, NSMP *ARID1A* wild-type, β -CATabn groups show a favorable prognosis, MMRd tumors have an intermediate outcome, while patients with either p53abn or NSMP with *ARID1A* mutation (NSMP_A) tumors feature a worse prognosis and are associated with a higher rate of recurrence (log-rank: $\chi^2 = 14.07$, P-value = 0.029). As regards the overall survival, the statistical significance is borderline ($\chi^2 = 12.60$, P-value = 0.050) (see figures 12a and 12b).

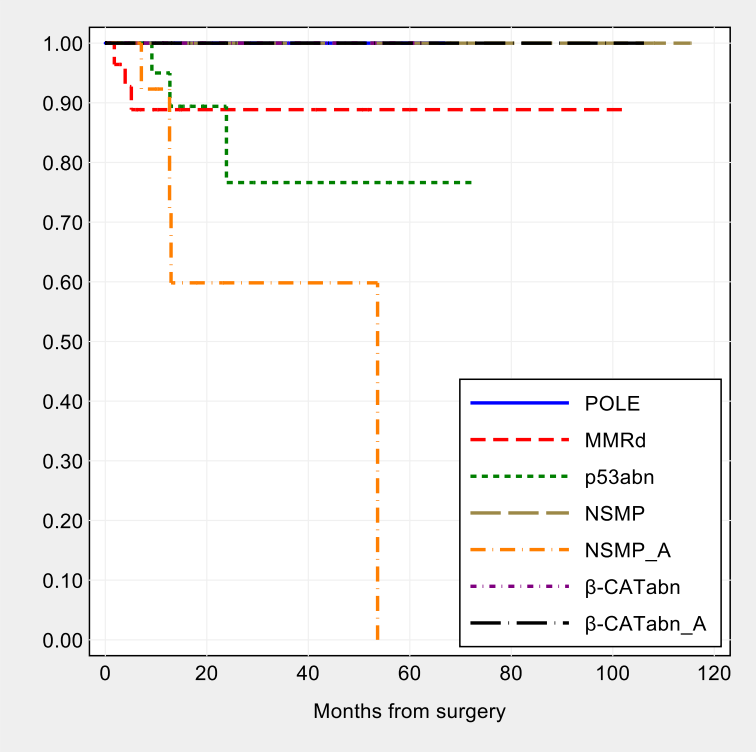

Figure 12a. Kaplan–Meier estimates of disease-free survival in patients at high-intermediate and high risk according to ESMO (n = 99), by molecular subgroup including β-catenin and *ARID1A* alterations.

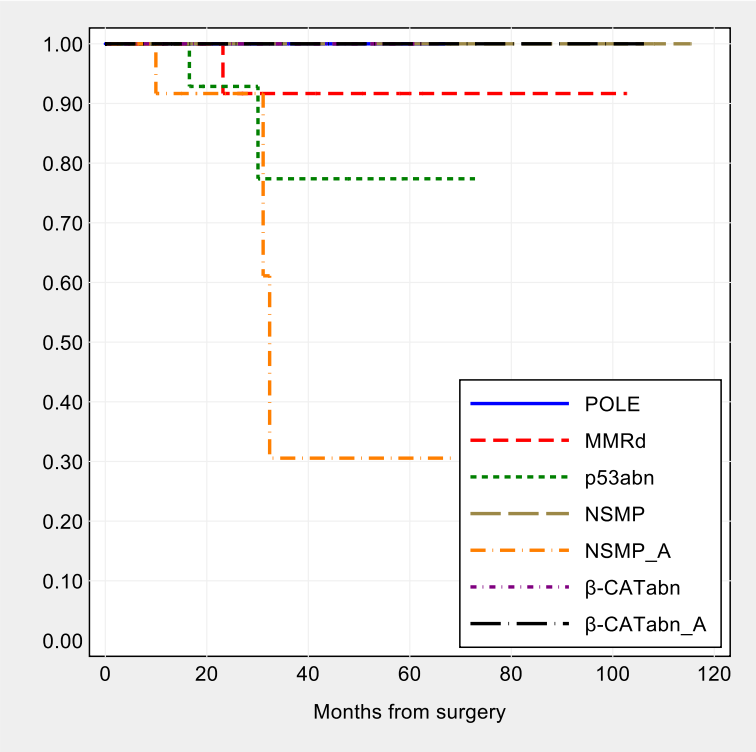

Figure 12b. Kaplan–Meier estimates of overall survival in patients at high-intermediate and high risk according to ESMO (n = 99), by molecular subgroup, including β-catenin and *ARID1A* alterations.

Discussion

In 2013, the multi-institutional TCGA project identified four distinct prognostic groups for the molecular classification of endometrial carcinoma. The TCGA study stratified EC into clinically low-risk (*POLE*-ultramutated), intermediate-risk (copy-number low/NSMP and hypermutated/MMRd groups) and high-risk (copy-number high/p53 mutant group) categories.

Subsequently, two studies (ProMisE and PORTEC) have developed and validated molecular classification tools based on widely accessible surrogate markers capable of discriminating four molecular EC subclasses with distinct prognostic outcomes, analogous - but not identical to those outlined in the TCGA study. In contrast to the previous multitude of biomarkers reported in literature, these routine molecular classifiers provide biologically relevant information that is potentially useful for both research and clinical applications to better stratify ECs.

In spite of the prognostic value of the novel molecular classification, the so-called copy number low/ No Specific Molecular Profile (NSMP) group represents the majority of ECs with intra-class heterogeneity in terms of biological behavior and clinical outcomes. In the NSMP group the presence of chromosome 1q amplification, *CTNNB1* mutations, and L1CAM expression may predict an increased risk for recurrence. Activating mutations in exon 3 of *CTNNB1* are likely early drivers in endometrial carcinogenesis and are identified in a significant proportion (26 – 52%) of NSMP cases. For these reasons, *CTNNB1*-mutated ECs may be regarded as a fifth molecular group.

In this study we investigated the feasibility of the surrogate TCGA molecular classification in our cohort of EC patients correlating it to conventional clinicopathologic characteristics. To analyze the prognostic heterogeneity of the NSMP tumors, we also aimed to explore the significance of *CTNNB1* and *ARID1A* alterations in this EC group by assessing their impact on disease recurrence and clinicopathologic characteristics.

A limitation of our study is the relatively low number of cases and the fact that the study is retrospective and from a single institution. However, meticulous histopathologic analysis and the use of whole tumor sections (as opposed to biopsy samples) for molecular and immunohistochemical analyses to avoid biases due to tumor heterogeneity insure the validity of our results.

Interestingly, in our EC series the FIGO stage has proved to be a robust parameter, being strongly correlated to both disease-free survival and overall survival. In addition, the integration of conventional clinicopathological parameters according to ESMO 2016 criteria has allowed to divide our EC series into different risk groups statistically related to recurrence.

Applying surrogate TCGA classification, our data confirm the previously reported distribution of the four molecular groups of endometrial carcinoma [48-50, 52]. *POLE* mutated tumors constitute about 10% of our EC cohort and are associated with excellent outcome. They are characterized by high grade, low stage, specific myometrial invasion patterns (MELF and tumor budding), intense intra- and peri-tumoral lymphocytic infiltrate, and high proliferative activity. We confirm the link reported in other studies between *POLE* tumors and lower BMI, although in our series there is no statistical association to young age at the time of diagnosis [53].

The MMRd group (approximately 30% of our cases) shows morphological characteristics similar to those of the *POLE* group, such as endometrioid-type histology and abundance of tumor-infiltrating lymphocytes. However, MMRd ECs have an intermediate prognosis, which significantly differs from that of the *POLE* group tumors.

Tumors of the p53 abnormal group (approximately 20% in our series) have aggressive histologic characteristics including high grade, non-endometrioid features, and significantly higher FIGO stage.

NSMP ECs represent approximately 40% of the cases in our cohort and are predominantly low-grade endometrioid carcinomas with low proliferative activity.

Although our results are consistent with literature, the classification into four molecular TCGA groups alone did not achieve statistical significance in prognostic stratification.

Our study was not limited only to surrogate TCGA subtyping, but it also aimed to investigate the relevance of *ARID1A* and *CTNNB1* mutations and their predictive-prognostic impact with particular reference to the NSMP group.

CTNNB1 mutations/β-catenin abnormal expression (found in approximately 20% of NSMP tumors) identify a subset characterized by young age at diagnosis, high BMI, low mitotic rate and low Ki67 proliferative index, and low TILs counts. As reported in the literature, *CTNNB1* mutated tumors are predominantly low grade and low stage, but in our cohort this molecular alteration is not linked to unfavorable prognosis.

A relevant finding of our study is the definition of the clinical and prognostic impact of *ARID1A* alterations. ARID1A normally maintains endometrial epithelial cell identity by repressing mesenchymal cell fates. A recent study has shown that coexistent *ARID1A* and *PI3K* mutations promote epithelial transdifferentiation associated with epithelial-to-mesenchymal transition (EMT). These findings support a tumor suppressor role for ARID1A-containing SWI/SNF complexes, so its loss-of-function may increase the EC invasive potential. Previous studies have also shown that *ARID1A* alteration is strongly associated with sporadic mismatch repair loss [27, 28], suggesting that by having a role in epigenetic silencing of *MLH1, ARID1A* is a causative, instead of a target gene for microsatellite instability. However, in our MMRd group, ARID1A loss is usually a subclonal event - both by IHC and NGS - suggesting that the alteration of *ARID1A* follows, instead of preceding microsatellite instability. In our study we have confirmed that *ARID1A* alterations occur in both MMRd as well as *POLE* group tumors, while they are inversely related to p53 mutated tumors. In the entire cohort, *ARID1A* mutated carcinomas are prevalently endometrioid, undifferentiated/dedifferentiated and exhibit histopathologic features such as MELF, presence of TILs and high proliferative index. We have explored the role of *ARID1A* in the β-

catenin altered and NSMP subgroups to determine its impact on clinical features and prognosis. In both subgroups *ARID1A* alteration is associated with novel and distinctive histological features: (1) in β-catenin altered tumors ARID1A loss correlates with high histologic-grade, necrosis, tumor budding, TILs and high proliferative activity; (2) in the NSMP group, *ARID1A* mutation correlates with increased proliferative activity and, interestingly, it identified all NSMP with recurrent disease. This remarkable finding can improve the surrogate molecular EC classification differentiating the biological heterogeneity of NSMP tumors and identifying a subset of ECs (NSMP_A) at higher risk of relapse. By integrating conventional ESMO 2016 clinicopathologic criteria and narrowing the analysis to high risk groups, our immuno-molecular classifier implemented with β-catenin and *ARID1A* alterations proved to be statistically associated with recurrence. In order to test the performance of our immuno-molecular classification with an external case series we tried our algorithm using TCGA data (see Supplementary Figure 1). The log-rank test showed a trend for both overall and disease-free survival (p-value of 0.069 and of 0.081, respectively), indicating conformity with TCGA data. However, as also shown in previous studies, surrogate molecular classification is similar to - but does not simply overlap with - the TCGA scheme for endometrial cancer [16-18]. In particular, we – unlike TCGA – have selected high-risk cases according to ESMO criteria based on clinicopathologic features and then tested material from these cases for *ARID1A* and *CTNNB1*/β-catenin. In addition, our study has included immunohistochemical analysis for ARID1A on whole slides in order to identify subclones and to guide subsequent molecular sequencing. Moreover, our cases have been enrolled consecutively, without selection bias, from a referral center for gynecologic oncology, with survival time and follow-up different from the TCGA cases. These points may explain some of the differences in survival patterns when our classifier is applied to TCGA data (see Supplementary Figure 1).

The multistep classification approach proposed in our study allows to better discriminate NSMP tumors by the simple addition of two markers to the already known PORTEC/ProMisE algorithms. In particular,

the assessment of *ARID1A* in NSMP group could change the clinical management of these patients: i.e. a closer follow-up could be proposed for an early detection of possible recurrence. In addition, ARID1A is emerging as a potential therapeutic target. Recent studies have showed that ARID1A loss is associated with improved response to immunotherapy across diverse tumor types [44, 45]. Considering these observations, the presence of *ARID1A* alterations may enable better patient selection who benefit from immune checkpoint blockade, also in non-*POLE*/MMRd tumors.

Conclusions

The evolution of EC classification from being purely based on morphology, to classification incorporating molecular profile promises for more accurately subtyping endometrial carcinoma to better reflect patient prognosis and outcome. This study confirms the feasibility of surrogate molecular TCGA classification of EC into routine clinical practice. Our immuno-molecular classification scheme supplemented with NSMP tumor sub-grouping based on the *CTNNB1* and *ARID1A* status granted a more reliable risk assessment and it resulted to be particularly informative in the group of high-risk patients. Our data indicates that *ARID1A* analysis may be a useful biomarker to identify patients who have worse prognosis in the NSMP group and may therefore require more aggressive forms of treatment and closer follow up. However, this classifier does not replace risk assessment based on conventional clinicopathologic parameters that will remain essential in prognostic stratification (i.e. FIGO stage). It is reasonable that molecular and clinicopathologic prognostic grouping systems will likely work better together.

Acknowledgments

I would like to thank all group members of the Research Center for Gynecologic Cancer (Centro di Studio e Ricerca sulle Neoplasie Ginecologiche) at the University of Bologna Medical Center, for the scientific advice.

References

1. Ferlay J, Colombet M, Soerjomataram I, Dyba T, Randi G, Bettio M, et al. Cancer incidence and mortality patterns in Europe: Estimates for 40 countries and 25 major cancers in 2018. Eur J Cancer. 2018;103:356-87.

2. Allemani C, Matsuda T, Di Carlo V, Harewood R, Matz M, Niksic M, et al. Global surveillance of trends in cancer survival 2000-14 (CONCORD-3): analysis of individual records for 37 513 025 patients diagnosed with one of 18 cancers from 322 population-based registries in 71 countries. Lancet. 2018;391:1023-75.

3. Group AW. I numeri del cancro in Italia. http://www.registri-tumori.it/PDF/AIOM2018/I_numeri_del_cancro_2018.pdf. 2018.

4. Quaresma M, Coleman MP, Rachet B. 40-year trends in an index of survival for all cancers combined and survival adjusted for age and sex for each cancer in England and Wales, 1971-2011: a population-based study. Lancet. 2015;385:1206-18.

5. Bokhman JV. Two pathogenetic types of endometrial carcinoma. Gynecol Oncol. 1983;15:10-7.

6. Dondi G, Coluccelli S, De Leo A, Ferrari S, Gruppioni E, Bovicelli A, et al. An Analysis of Clinical, Surgical, Pathological and Molecular Characteristics of Endometrial Cancer According to Mismatch Repair Status. A Multidisciplinary Approach. Int J Mol Sci. 2020;21.

7. Committee on Practice B-G, Society of Gynecologic O. ACOG Practice Bulletin No. 147: Lynch syndrome. Obstet Gynecol. 2014;124:1042-54.

8. Giardiello FM, Allen JI, Axilbund JE, Boland CR, Burke CA, Burt RW, et al. Guidelines on genetic evaluation and management of Lynch syndrome: a consensus statement by the US Multi-Society Task Force on colorectal cancer. Gastroenterology. 2014;147:502-26.

9. Provenzale D, Gupta S, Ahnen DJ, Bray T, Cannon JA, Cooper G, et al. Genetic/Familial High-Risk Assessment: Colorectal Version 1.2016, NCCN Clinical Practice Guidelines in Oncology. J Natl Compr Canc Netw. 2016;14:1010-30.

10. The WHO Classification of Tumours Editorial Board. WHO Classification of Tumours, Female Genital Tumours, 5th Edition, Volume 4 5th Edition, Volume 4. IARC: Lyon, France, 2020.

11. Nielsen AL, Thomsen HK, Nyholm HC. Evaluation of the reproducibility of the revised 1988 International Federation of Gynecology and Obstetrics grading system of endometrial cancers with special emphasis on nuclear grading. Cancer. 1991;68:2303-9.

12. Pecorelli S. Revised FIGO staging for carcinoma of the vulva, cervix, and endometrium. Int J Gynaecol Obstet. 2009;105:103-4.

13. Amin MB, Edge S, Greene F, Byrd DR, Brookland RK, Washington MK, et al. AJCC Cancer Staging Manual (8th edition). 2017.

14. Colombo N, Creutzberg C, Amant F, Bosse T, Gonzalez-Martin A, Ledermann J, et al. ESMO-ESGO-ESTRO Consensus Conference on Endometrial Cancer: diagnosis, treatment and follow-up. Ann Oncol. 2016;27:16-41.

15. Cancer Genome Atlas Research N, Kandoth C, Schultz N, Cherniack AD, Akbani R, Liu Y, et al. Integrated genomic characterization of endometrial carcinoma. Nature. 2013;497:67-73.

16. Stelloo E, Nout RA, Osse EM, Jurgenliemk-Schulz IJ, Jobsen JJ, Lutgens LC, et al. Improved Risk Assessment by Integrating Molecular and Clinicopathological Factors in Early-stage Endometrial Cancer-Combined Analysis of the PORTEC Cohorts. Clin Cancer Res. 2016;22:4215-24.

17. Talhouk A, McConechy MK, Leung S, Li-Chang HH, Kwon JS, Melnyk N, et al. A clinically applicable molecular-based classification for endometrial cancers. Br J Cancer. 2015;113:299-310.

18. Talhouk A, McConechy MK, Leung S, Yang W, Lum A, Senz J, et al. Confirmation of ProMisE: A simple, genomics-based clinical classifier for endometrial cancer. Cancer. 2017;123:802-13.

19. Kurnit KC, Kim GN, Fellman BM, Urbauer DL, Mills GB, Zhang W, et al. CTNNB1 (beta-catenin) mutation identifies low grade, early stage endometrial cancer patients at increased risk of recurrence. Mod Pathol. 2017;30:1032-41.

20. Liu Y, Patel L, Mills GB, Lu KH, Sood AK, Ding L, et al. Clinical significance of CTNNB1 mutation and Wnt pathway activation in endometrioid endometrial carcinoma. J Natl Cancer Inst. 2014;106.

21. Wilson BG, Roberts CW. SWI/SNF nucleosome remodellers and cancer. Nat Rev Cancer. 2011;11:481-92.

22. Shen J, Peng Y, Wei L, Zhang W, Yang L, Lan L, et al. ARID1A Deficiency Impairs the DNA Damage Checkpoint and Sensitizes Cells to PARP Inhibitors. Cancer Discov. 2015;5:752-67.

23. Mathur R. ARID1A loss in cancer: Towards a mechanistic understanding. Pharmacol Ther. 2018;190:15-23.

24. Guan B, Mao TL, Panuganti PK, Kuhn E, Kurman RJ, Maeda D, et al. Mutation and loss of expression of ARID1A in uterine low-grade endometrioid carcinoma. Am J Surg Pathol. 2011;35:625-32.

25. Rahman M, Nakayama K, Rahman MT, Katagiri H, Katagiri A, Ishibashi T, et al. Clinicopathologic analysis of loss of AT-rich interactive domain 1A expression in endometrial cancer. Hum Pathol. 2013;44:103-9.

26. Wiegand KC, Lee AF, Al-Agha OM, Chow C, Kalloger SE, Scott DW, et al. Loss of BAF250a (ARID1A) is frequent in high-grade endometrial carcinomas. J Pathol. 2011;224:328-33.

27. Allo G, Bernardini MQ, Wu RC, Shih Ie M, Kalloger S, Pollett A, et al. ARID1A loss correlates with mismatch repair deficiency and intact p53 expression in high-grade endometrial carcinomas. Mod Pathol. 2014;27:255-61.

28. Bosse T, ter Haar NT, Seeber LM, v Diest PJ, Hes FJ, Vasen HF, et al. Loss of ARID1A expression and its relationship with PI3K-Akt pathway alterations, TP53 and microsatellite instability in endometrial cancer. Mod Pathol. 2013;26:1525-35.

29. Yen TT, Miyamoto T, Asaka S, Chui MH, Wang Y, Lin SF, et al. Loss of ARID1A expression in endometrial samplings is associated with the risk of endometrial carcinoma. Gynecol Oncol. 2018;150:426-31.

30. Wilson MR, Reske JJ, Holladay J, Wilber GE, Rhodes M, Koeman J, et al. ARID1A and PI3-kinase pathway mutations in the endometrium drive epithelial transdifferentiation and collective invasion. Nat Commun. 2019;10:3554.

31. Gilks CB, Oliva E, Soslow RA. Poor interobserver reproducibility in the diagnosis of high-grade endometrial carcinoma. Am J Surg Pathol. 2013;37:874-81.

32. Perrone AM, Di Marcoberardino B, Rossi M, Pozzati F, Pellegrini A, Procaccini M, et al. Laparoscopic versus laparotomic approach to endometrial cancer. Eur J Gynaecol Oncol. 2012;33:376-81.

33. Kurman RJ, Carcangiu ML, Herrington S, Young RH. WHO Classification of Tumours of Female Reproductive Organs 4th edn. IARC: Lyon, France, 2014.

34. FIGO: 27(th) volume of the ANNUAL REPORT on the Results of Treatment in Gynecological Cancer. Int J Gynaecol Obstet. 2006;95 Suppl 1:xxiii.

35. Murray SK, Young RH, Scully RE. Unusual epithelial and stromal changes in myoinvasive endometrioid adenocarcinoma: a study of their frequency, associated diagnostic problems, and prognostic significance. Int J Gynecol Pathol. 2003;22:324-33.

36. Euscher E, Fox P, Bassett R, Al-Ghawi H, Ali-Fehmi R, Barbuto D, et al. The pattern of myometrial invasion as a predictor of lymph node metastasis or extrauterine disease in low-grade endometrial carcinoma. Am J Surg Pathol. 2013;37:1728-36.

37. Bosse T, Peters EE, Creutzberg CL, Jurgenliemk-Schulz IM, Jobsen JJ, Mens JW, et al. Substantial lymph-vascular space invasion (LVSI) is a significant risk factor for recurrence in endometrial cancer--A pooled analysis of PORTEC 1 and 2 trials. Eur J Cancer. 2015;51:1742-50.

38. Fujimoto T, Nanjyo H, Fukuda J, Nakamura A, Mizunuma H, Yaegashi N, et al. Endometrioid uterine cancer: histopathological risk factors of local and distant recurrence. Gynecol Oncol. 2009;112:342-7.

39. Shia J, Black D, Hummer AJ, Boyd J, Soslow RA. Routinely assessed morphological features correlate with microsatellite instability status in endometrial cancer. Hum Pathol. 2008;39:116-25.

40. Hendry S, Salgado R, Gevaert T, Russell PA, John T, Thapa B, et al. Assessing Tumor-Infiltrating Lymphocytes in Solid Tumors: A Practical Review for Pathologists and Proposal for a Standardized Method from the International Immuno-Oncology Biomarkers Working Group: Part 2: TILs in Melanoma, Gastrointestinal Tract Carcinomas, Non-Small Cell Lung Carcinoma and Mesothelioma, Endometrial and Ovarian Carcinomas, Squamous Cell Carcinoma of the Head and Neck, Genitourinary Carcinomas, and Primary Brain Tumors. Adv Anat Pathol. 2017;24:311-35.

41. Singh N, Piskorz AM, Bosse T, Jimenez-Linan M, Rous B, Brenton JD, et al. p53 immunohistochemistry is an accurate surrogate for TP53 mutational analysis in endometrial carcinoma biopsies. J Pathol. 2020;250:336-45.

42. Garg K, Broaddus RR, Soslow RA, Urbauer DL, Levine DA, Djordjevic B. Pathologic scoring of PTEN immunohistochemistry in endometrial carcinoma is highly reproducible. Int J Gynecol Pathol. 2012;31:48-56.

43. Nei H, Saito T, Yamasaki H, Mizumoto H, Ito E, Kudo R. Nuclear localization of beta-catenin in normal and carcinogenic endometrium. Mol Carcinog. 1999;25:207-18.

44. Travaglino A, Raffone A, Saccone G, De Luca C, Mollo A, Mascolo M, et al. Immunohistochemical Nuclear Expression of beta-Catenin as a Surrogate of CTNNB1 Exon 3 Mutation in Endometrial Cancer. Am J Clin Pathol. 2019;151:529-38.

45. de Biase D, Acquaviva G, Visani M, Sanza V, Argento CM, De Leo A, et al. Molecular Diagnostic of Solid Tumor Using a Next Generation Sequencing Custom-Designed Multi-Gene Panel. Diagnostics (Basel). 2020;10.

46. van Roon EH, van Puijenbroek M, Middeldorp A, van Eijk R, de Meijer EJ, Erasmus D, et al. Early onset MSI-H colon cancer with MLH1 promoter methylation, is there a genetic predisposition? BMC Cancer. 2010;10:180.

47. Leon-Castillo A, Britton H, McConechy MK, McAlpine JN, Nout R, Kommoss S, et al. Interpretation of somatic POLE mutations in endometrial carcinoma. J Pathol. 2020;250:323-35.

48. Kommoss S, McConechy MK, Kommoss F, Leung S, Bunz A, Magrill J, et al. Final validation of the ProMisE molecular classifier for endometrial carcinoma in a large population-based case series. Ann Oncol. 2018;29:1180-8.

49. Raffone A, Travaglino A, Mascolo M, Carbone L, Guida M, Insabato L, et al. TCGA molecular groups of endometrial cancer: Pooled data about prognosis. Gynecol Oncol. 2019;155:374-83.

50. Stelloo E, Bosse T, Nout RA, MacKay HJ, Church DN, Nijman HW, et al. Refining prognosis and identifying targetable pathways for high-risk endometrial cancer; a TransPORTEC initiative. Mod Pathol. 2015;28:836-44.

51. Kim G, Kurnit KC, Djordjevic B, Singh C, Munsell MF, Wang WL, et al. Nuclear beta-catenin localization and mutation of the CTNNB1 gene: a context-dependent association. Mod Pathol. 2018;31:1553-9.

52. Espinosa I, De Leo A, D'Angelo E, Rosa-Rosa JM, Corominas M, Gonzalez A, et al. Dedifferentiated endometrial carcinomas with neuroendocrine features: a clinicopathologic, immunohistochemical, and molecular genetic study. Hum Pathol. 2018;72:100-6.

53. Roque DR, Makowski L, Chen TH, Rashid N, Hayes DN, Bae-Jump V. Association between differential gene expression and body mass index among endometrial cancers from The Cancer Genome Atlas Project. Gynecol Oncol. 2016;142:317-22.

Supplementary materials

Supplementary Table 1: List of antibodies

Antibody	Source	Dilution	Method
Mouse anti-β-Catenin, clone 14	Cell Marque, USA	RTU	UltraCC1 x 32' at 95°C - Ab 16' at 36°C
Rabbit anti-PTEN, clone SP218	Ventana, USA	RTU	UltraCC1 x 56' at 100°C - Ab 16' at 36°C
Rabbit anti-ARID1A polyclonal	Atlas antibodies	1:90	UltraCC1 x 32' at 95°C - Ab 32' at 36°C
Mouse anti-p53, clone DO7	Ventana, USA	RTU	UltraCC1 x 24' at 95°C - Ab 12' at 36°C
Mouse anti-MLH1, clone M1	Ventana, USA	RTU	UltraCC1 x 56' at 98°C - Ab 32' at 36°C
Mouse anti-PMS2, clone A16-4	Ventana, USA	RTU	UltraCC1 x 64' at 99°C - Ab 32' at 36°C
Mouse anti-MSH2, clone G219-1129	Ventana, USA	RTU	UltraCC1 x 56' at 95°C - Ab 32' at 36°C
Rabbit anti-MSH6, clone SP93	Ventana, USA	RTU	UltraCC1 x 64' at 100°C - Ab 12' at 36°C
Rabbit anti-Ki67, clone 30-9	Ventana, USA	RTU	UltraCC1 x 32' at 99°C - Ab 8' at RT

Visualization with OptiView DAB Detection kit, Ventana, USA

Supplementary Table 2: List of variants identified by Next Generation Sequencing

POLE	*TP53*	*PIK3CA*	*KRAS*	*CTNNB1*	*ARID1A*
M444K	T155P	E542K	A59T	G34R	E596H
R375W	F109V - R213Ter	H1047R	G12D	G34V	A226D
A456P	G245S	H1047Y	G12V	D32Y	A900T
V411L	L201Fs	I1058L	G13D	S33C	G768D
P286R	S241F	L1001I	Q61H	T41I	L1100F-R1446Q-R1989Ter
P286R - F366L	R213Ter	M1043I		S45Del	S530Fs
P286R	R282Del	N1044S			G455E
F367C	R273H	N1068Fs			P728Fs
P436H	Y327Ter	P539R			N209S
	D281E - S149Fs	T1025A			R1833C
	I195T	Y1021C			c.3867-15T>C
					R1906Q
					R1722Ter
					P554Q
					c.2420-18G>C
					K996Fs
					Q1519Fs
					R693Ter
					S2262Fs
					R219H
					I1691Fs
					R1989Ter
					P146Fs
					A985Fs - R1335Ter
					P554Q - Y1279Ter
					Y401Ter-G1762E_insE
					R1721Ter - Q2210Ter
					L1092Ter
					G240AFsTer121
					Q586Ter

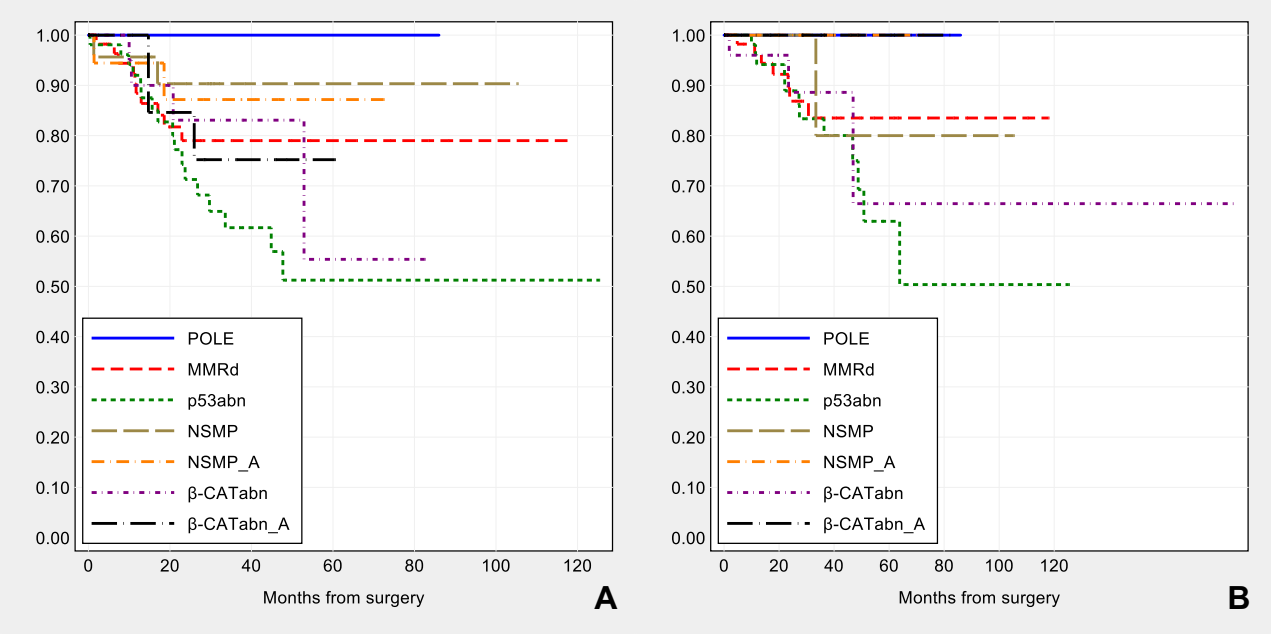

Supplementary Figure 1. Kaplan–Meier estimates of disease-free survival (A) and overall survival (B) in TCGA case series, by molecular subgroup including β-catenin and *ARID1A* alterations (A: log-rank $\chi^2 = 11.24$, P-value = 0.081; B: log-rank $\chi^2 = 11.69$, P-value = 0.069).